EUROPEAN ORGANIZATION FOR NUCLEAR RESEARCH (CERN)

CERN-EP-2026-080
2026/09/14

CMS-HIG-24-003

Search for associated production of a Higgs boson and two vector bosons via vector boson scattering at $\sqrt{s} = 13\,\text{TeV}$

The CMS Collaboration*

arXiv:2604.24531v2 [hep-ex] 10 Sep 2026

Abstract

A search for Higgs boson (H) production in association with two vector bosons (V = W, Z) via vector boson scattering (VBS) is presented using proton-proton collision data collected at $\sqrt{s} = 13\,\text{TeV}$ by the CMS experiment, corresponding to an integrated luminosity of $138\,\text{fb}^{-1}$. Events containing two forward jets consistent with VBS, a large-radius jet from the decay of a boosted H to a pair of b quarks, and 0, 1, or 2 charged leptons coming from V decays are selected. The process is excluded at 95%CL for observed (expected) values of the VVHH coupling modifier κ_{2V} outside the interval $0.40 < \kappa_{2V} < 1.60$ ($0.34 < \kappa_{2V} < 1.66$), assuming standard model values for all other couplings, thus establishing a novel probe of the VVHH interaction. Constraints are also set on the individual κ_{2W} and κ_{2Z} coupling modifiers, and on the allowed region in the κ_{2W}-κ_{2Z} plane.

Published in Physical Review Letters as doi:10.1103/gwj9-5bxm.

© 2026 CERN for the benefit of the CMS Collaboration. CC-BY-4.0 license

*See Appendix C for the list of collaboration members

The discovery of the Higgs boson (H) by the ATLAS and CMS Collaborations at the CERN LHC in 2012 [1–3] marked a milestone in our understanding of fundamental interactions. Since then, extensive efforts have focused on measuring its properties and couplings. The H self-coupling and the VVHH (V = W, Z) quartic coupling, the modifiers of which with respect to the standard model (SM) are parametrized as κ_λ and κ_{2V} [4, 5], respectively, have so far been probed only in searches for H pair production [6, 7]. An alternative path to access both these couplings is offered by H production in association with a pair of vector bosons (VVH) via vector boson scattering (VBS). This is illustrated in Fig. 1, where two of the leading order (LO) Feynman diagrams are shown.

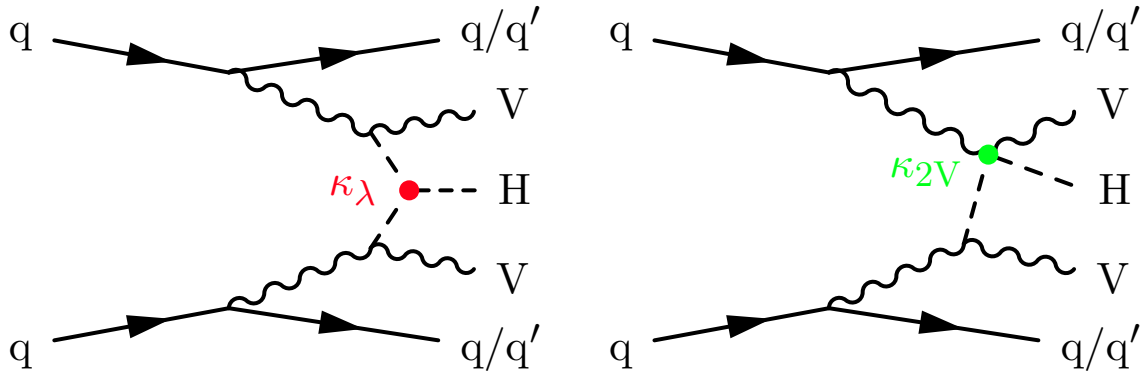

Figure 1: Examples of tree-level Feynman diagrams for the production of VVH via VBS, with dependencies on the H self-coupling (left) and the VVHH quartic coupling (right). The corresponding vertices are denoted by the κ_λ and κ_{2V} modifiers, respectively.

The VBS VVH production cross section at $\sqrt{s}$ = 13 TeV is predicted to be 1.99 fb at LO [8], considering all the relevant processes. However, deviations in κ_{2V} from the SM value of 1 can significantly enhance the cross section and boost the final-state objects, thereby increasing the experimental sensitivity to this process. This makes the search for VBS VVH production synergistic with H pair production searches, which constrain κ_{2V} within the range of $[0.64, 1.40]$ using CMS data collected at $\sqrt{s} = 13$ TeV [6]. ATLAS data constrain the same parameter in the range $[0.6, 1.5]$ [7]. More recently, a CMS search for H pair production in final states with four b quarks constrained κ_{2V} in the range $[0.74, 1.30]$, using improved b tagging algorithms and combining data collected at 13 and 13.6 TeV [9]. The VBS VVH production is also sensitive to the individual WWHH and ZZHH couplings, with modifiers κ_{2W} and κ_{2Z} are only loosely constrained by the CMS search for VHH production [10]. Deviations in κ_λ determine less pronounced changes in cross section and kinematics. Consequently, the exploration of the H self-coupling is left to future work, and $\kappa_\lambda = 1$ is assumed in this search.

This Letter reports on a search for VVH production via VBS in proton-proton collision data at $\sqrt{s} = 13$ TeV collected by the CMS experiment at the LHC in 2016–2018, corresponding to an integrated luminosity of 138 fb^{-1}. The search is performed in several channels: all-hadronic, single-lepton, and dilepton, depending on the number of reconstructed leptons (ℓ) from the W or the Z boson decays. Dilepton channels target final states containing electrons and muons with charges of the same or opposite sign (SS or OS). Events with one hadronically decaying τ lepton are also accepted in the SS channel. Final states where the H decays into a pair of b quarks are studied. A large Lorentz boost is required for the decay products of the H and the vector bosons. Therefore, the H and at least one vector boson decaying hadronically, if present, are reconstructed as single large-radius jets. All channels utilize the characteristic VBS signature of two additional jets with a large pseudorapidity (η) separation.

The CMS apparatus [11, 12] is a multipurpose, nearly hermetic detector, designed to trigger on [13–15] and identify electrons, muons, photons, and hadrons [16–18]. The CMS "particle-flow" (PF) algorithm [19] combines the information provided by the all-silicon tracker and by the crystal electromagnetic (ECAL) and brass-scintillator hadron calorimeters (HCAL), operating inside a 3.8 T superconducting solenoid, with data from the gas-ionization muon detectors embedded in the flux-return yoke outside the solenoid, to reconstruct individual particles, which are further used to build τ leptons, jets, and missing transverse momentum [20–22]. The primary vertex (PV) is chosen as the vertex corresponding to the hardest scattering in the event, evaluated using tracking information alone [23].

Muon candidates are reconstructed within $|\eta| < 2.4$ by combining silicon tracker and muon chamber data [17]. Muons must meet quality criteria based on tracker and muon detector hits, track properties, and impact parameters relative to the PV. Electron candidates within $|\eta| < 2.5$ are reconstructed by matching silicon tracker tracks to ECAL energy clusters [16]. They must meet identification criteria based on shower cluster shape, track-cluster matching, HCAL energy fraction, and track compatibility with the PV. Electrons in the ECAL barrel-endcap transition region ($1.44 < |\eta| < 1.57$) or originating from photon conversions are discarded. The lepton isolation is computed by summing the transverse momenta (p_T) of PF candidates originating from the PV within a cone of $\Delta R = \sqrt{(\Delta\eta)^2 + (\Delta\phi)^2} = 0.4\,(0.3)$ around the muon (electron), where ϕ is the azimuthal angle, and is corrected for the contribution of neutral particles from additional interactions in the same or nearby bunch crossings (pileup) [16, 17, 24]. Selections are based on the isolation sum normalized to the p_T of the lepton. Leptons are classified as "tight" or "loose" according to the criteria defined in Ref. [25] in all channels, except for the SS dilepton channel, where criteria similar to those defined in Refs. [16, 17, 24] are used. Hadronically decaying τ leptons are identified by the DEEPTAU algorithm [26].

Jets are clustered from PF candidates using the anti-k_T algorithm [27, 28]. Distance parameters of 0.4 and 0.8 are used to reconstruct so-called "AK4" and "AK8" (or large-radius) jets, respectively. Jet momenta are corrected to reduce pileup contributions: the charged hadron subtraction [29] and the pileup-per-particle identification [29, 30] algorithms are used for AK4 and AK8 jets, respectively. Further corrections are derived from simulation and in-situ measurements in data [21]. Jets affected by detector noise or reconstruction failures are discarded, and pileup jets are suppressed using a multivariate discriminator [29]. The missing transverse momentum vector, $\vec{p}_T^{\,\text{miss}}$, with magnitude p_T^{miss}, is defined as the negative $\vec{p}_T$ sum of all PF candidates and corrected for AK4 jet energy scale calibrations [22].

The mass-decorrelated version of the $X \to b\bar{b}$ PARTICLENET tagger [31] is used to identify $H \to b\bar{b}$ candidates with a mass-independent probability score ranging from 0 to 1. An analogously mass-decorrelated $X \to qq$ PARTICLENET tagger identifies hadronic vector boson decays. To estimate the AK8 jet mass, the "soft-drop" (SD) grooming algorithm [32–34] with $\beta = 0$ and $z = 0.1$ is applied, yielding the SD mass, m_{SD}. The AK8 mass resolution is further improved using the PARTICLENET-regressed mass, m_{PN}. For boosted H and vector boson reconstruction, AK8 jets with $|\eta| < 2.5$, ungroomed mass > 50 GeV, and $m_{SD} > 40$ GeV are considered. After selecting AK8 jets, nonoverlapping AK4 jets are used for b and VBS jet identification. The AK4 jets originating from b quarks within $|\eta| < 2.5$ are identified using the DEEPJET [35–37] algorithm and are used to suppress the background arising from $t\bar{t}$ production. Jets are classified as b jets based on the DEEPJET output, with loose, medium, and tight working points corresponding to light-flavor quark or gluon jet misidentification rates of 10, 1, and 0.1%, and efficiencies of about 92, 75, and 58%, respectively. The AK4 jets with $p_T > 30$ GeV and $|\eta| < 4.7$ are considered as VBS jet candidates.

We model VBS VVH events and calculate the corresponding production cross sections at LO using the MADGRAPH5_aMC@NLO v2.6.5 [8] Monte Carlo event generator. The generator is interfaced with PYTHIA v8.240 [38] for the simulation of boson decays, using the dipole recoil scheme to correctly emulate the color structure [39]. To simulate events with different κ_{2V} values, the event reweighting feature of MADGRAPH5_aMC@NLO [40] is employed.

Background simulation is used in the optimization of the analysis, while data-driven methods are used for the purpose of modelling the data in all channels. Simulated events are also used in the SS dilepton channel to predict the SM background, in conjunction with control samples in data. The largest source of background in the all-hadronic channel is the production of multijet events through quantum chromodynamics (QCD) processes. The QCD background is simulated at LO with MADGRAPH5_aMC@NLO. Other major background processes are $\mathrm{t\bar{t}}$ and W + jets production. The $\mathrm{t\bar{t}}$ background [41] is simulated at next-to-LO (NLO) precision in perturbative QCD with the POWHEG v2.0 program [42–44]. The W + jets background is simulated with MADGRAPH5_aMC@NLO at LO, with up to four additional partons, merged at the parton shower level via the MLM matching scheme [45]. Other sources of background include diboson production, *s*-, *t*-channel and tW single top quark production, electroweak production of a W boson, quark-initiated WH, $\mathrm{t\bar{t}}$ + vector bosons, and Z + jets production.

The generated matrix-element-level events are interfaced with PYTHIA v8.240 to model parton showering and hadronization, as well as the underlying event. The generation of all samples is based on the CP5 tune [46] for PYTHIA and the NNPDF v3.1 next-to-NLO parton distribution functions (PDFs) [47, 48]. Simulated pileup interactions are added to the hard-scattering process, with a multiplicity matched to the pileup profiles of the data. The detector response is modeled with GEANT4 [49].

The search is performed across six channels, defined according to the lepton and jet multiplicities in the event. Events in the all-hadronic channel are required to contain exactly zero loose leptons, while in the single-lepton (dilepton) channel they must contain one (two) tight leptons. The all-hadronic channel is further split into two categories, semi-boosted and fully boosted, which require exactly two and more than two AK8 jets, respectively. The dilepton events are split into the OS and SS channels. Events in the OS dilepton channels are then categorized according to the dilepton mass ($m_{\ell\ell}$), requiring that it is either consistent with that of a Z boson (OS Z), or not (OS WW). All channels are orthogonal by construction except for the SS dilepton channel. For this channel the orthogonality is explicitly verified after the event selections are applied, because of the different lepton identification criteria employed.

In the all-hadronic channels, events of interest are collected using triggers based on the scalar p_{T} sum of all jets (H_{T}), with thresholds of 800 or 900 GeV for 2016, and 1050 GeV for 2017 and 2018. Events are split into the fully boosted and semi-boosted channels based on the number of AK8 jets with $p_{\mathrm{T}} > 300$ GeV. In the fully boosted channel, the $\mathrm{H} \to \mathrm{b\bar{b}}$ and both the vector boson candidates are reconstructed as AK8 jets. In the semi-boosted channel, one vector boson candidate is reconstructed as a pair of AK4 jets. In both channels, a pair of AK4 VBS jet candidates is also required: in the case of multiple pairs, the one with the largest absolute pseudorapidity difference ($|\Delta\eta_{\mathrm{jj}}|$) is selected.

In the single-lepton channel, single-lepton triggers require isolated leptons with $p_{\mathrm{T}} > 24$ (27) GeV for muons in 2016 and 2018 (2017), and $p_{\mathrm{T}} > 27$ (32) GeV for electrons in 2016 (2017–2018). Events must contain exactly one tight lepton with $p_{\mathrm{T}} > 40$ GeV and no additional loose leptons. Two AK8 jets with $p_{\mathrm{T}} > 250$ GeV are required and identified as the $\mathrm{H} \to \mathrm{b\bar{b}}$ and the hadronically decaying vector boson candidates. The VBS jets are chosen as the highest-momentum AK4 jets in opposite η regions. If this criterion fails, the two highest-momentum jets are se-

lected.

In the dilepton channels, single-lepton triggers are used for OS WW events. These are used in combination with dilepton triggers for OS Z events, with p_T thresholds of 17 and 8 GeV for muons, and 23 and 12 GeV for electrons. The SS dilepton channel also uses mixed muon-electron triggers, requiring a muon (electron) with $p_T > 23$ (12) GeV and an electron (muon) with $p_T > 23$ (8) GeV. Exactly two tight leptons are required, with no additional loose leptons. In the OS Z channel, the two leptons must have an invariant mass $m_{\ell\ell}$ consistent with that of a Z boson, requiring $86 < m_{\ell\ell} < 96$ GeV, while the same window is vetoed in the OS WW channel. The $H \to b\bar{b}$ candidate is reconstructed as an AK8 jet in all channels. In the OS Z channel, one vector boson decays hadronically and is also reconstructed as an AK8 jet. The VBS jet pair is chosen as the pair of AK4 jets with the largest $|\Delta\eta_{jj}|$ in both the OS channels, while the same selection as in the single-lepton channel is used in the SS channel.

An AK4 b jet veto is applied in the single-lepton and dilepton channels, to reduce the $t\bar{t}$ background contribution. Additional selection criteria on event properties are also applied, as summarized in Tables 1–6 in the End Matter.

A multivariate analysis is subsequently performed in all channels. Backgrounds are estimated from control samples in data using a matrix ("ABCD") method [50], except for the SS dilepton channel. The background in the signal region (A) is predicted from data in control regions B, C, and D, defined by inverting the criteria used to select the VBS jets (B), the VVH system (C), or both (D). This choice of the ABCD axes is motivated by the negligible correlation expected in background events between the properties of the VVH system and the VBS jets.

The all-hadronic and single-lepton channels use the method suggested in Ref. [51] to train a deep neural network (DNN) orthogonal to the discriminating features used to select the VBS jet pair. The output of the DNN and the VBS selection features are then used as the two ABCD axes. Different DNNs are trained in each channel, using simulated events to separate signal in the $\kappa_{2V} = 2$ benchmark scenario from all background sources. This benchmark is used as it is expected to be close to the final exclusion limit. In the all-hadronic fully boosted topology, the DNN uses as input the p_T, η, ϕ, and m_{PN} of the three selected AK8 jets, along with the invariant mass of the VBS jet pair, m_{jj}. A decorrelation term in the loss function ensures that the DNN output is independent of $\Delta\eta_{jj}$, and these same quantities are used to define the ABCD axes. After training, the minimum thresholds used to select on the $X \to b\bar{b}$ and $X \to qq$ PARTICLENET tagger scores are tightened for both the H and the vector boson candidates. The signal region A is defined by $|\Delta\eta_{jj}| > 5$ and a DNN output > 0.97. In the semi-boosted topology, the DNN is trained using the p_T, η, ϕ, and m_{SD} of the two selected AK8 jets, the four-vectors and the invariant mass m_{jj} of the AK4 jet pair forming the second vector boson candidate, and the p_T sum of all objects forming the VVH system, S_T. The DNN output is designed to be independent of $\Delta\eta_{jj}$. The signal region A is defined by requiring $|\Delta\eta_{jj}| > 6$, $m_{jj} > 1300$ GeV, and a DNN output > 0.8. In the single-lepton channel, the DNN inputs are the p_T and m_{PN} of the H and vector boson AK8 jets, the lepton p_T, the $m_{\ell b}$ variable, defined as the minimum invariant mass of the lepton and any b jet passing the loose DEEPJET tagger working point, and p_T^{miss}. Its output is constructed to be orthogonal to that of a boosted decision tree (BDT) used to select the VBS jet pair, trained on the p_T and η of the VBS jet candidates, $\Delta\eta_{jj}$ and m_{jj}. The signal region A is defined by requiring the DNN and BDT outputs to be > 0.9 and 0.82, respectively, with the $X \to b\bar{b}$ ($X \to qq$) tagger score > 0.5 (0.7).

In each dilepton channel, a BDT is trained to separate signal (in the $\kappa_{2V} = 2$ benchmark scenario) from simulated background. The BDTs are trained using features of the VVH system.

The absence of correlation with the properties of the VBS jets is verified after the training. In the OS WW channel, inputs include the H candidate p_T, η, m_{SD}; the p_T, η, flavor of each lepton; the $\Delta\eta$, ΔR, invariant mass of the two leptons; the event S_T and p_T^{miss}. The signal region A requires $m_{jj} > 760\,GeV$, $|\Delta\eta_{jj}| > 4.9$, a BDT score > 0.85, and an $X \to b\bar{b}$ tagger score > 0.7. In the OS Z channel, the BDT inputs are the p_T and η of the H and Z candidates, and of each lepton; the lepton impact parameter significances and isolation sums; and $m_{\ell\ell}$, the invariant mass of the VVH system, and S_T. The signal region A is defined by $m_{jj} > 750\,GeV$, $|\Delta\eta_{jj}| > 4$, and a BDT score > 0.85.

The selections used in each channel to define the signal region, or region A, are summarized in Table 7 in the End Matter, where the cuts inverted to define the B, C, D regions are also specified.

Systematic uncertainties in the background predictions are derived from closure tests in data. An analogous ABCD method is applied in data sidebands, and the prediction is compared to the observed data in the corresponding region A of the sideband. The uncertainty is estimated conservatively, by taking the relative difference in the worst closure sideband. Table 8 in the End Matter shows the data yields in the regions A, B, C and D, in each channel, alongside the predicted background with its uncertainties, and the benchmark signal expected in region A, for both the $\kappa_{2V} = 2$ and SM scenarios.

In the SS dilepton channel, a BDT is also trained to discriminate signal from background. The BDT inputs include the p_T and η of the $H \to b\bar{b}$ candidate; the p_T of the leptons; the momentum of the VBS jets and the p_T of the VBS dijet system; and $m_{\ell\ell}$, p_T^{miss}, S_T, and the scalar sum of the p_T of the leptons and p_T^{miss}. The signal region is then divided into three bins according to the BDT output score ($[0, 0.1]$, $[0.1, 0.25]$, $[0.25, 1]$).

Results are obtained via binned maximum likelihood fits of signal and background predictions to data [52], using the CMS COMBINE tool [53], based on the ROOFIT [54] and ROOSTATS [55] frameworks. In each channel, all the regions are fitted simultaneously, extracting the signal region predictions concurrently. Systematic uncertainties are included as nuisance parameters of the likelihood function and affect the signal and background normalization, except for the SS dilepton channel where shape variations are used. Experimental uncertainties in the signal acceptance are considered in the lepton trigger and identification efficiencies, jet energy scale and resolution [21], DEEPJET b tagging efficiency, PARTICLENET tagger efficiency, and integrated luminosity [56–58]. Theory uncertainties in the signal cross section include renormalization and factorization scales (μ_R and μ_F, respectively), PDFs, and initial- and final-state radiation modeling. The overall dominant systematic uncertainty, of approximately 25%, arises from μ_F, followed by the uncertainty arising from PDFs, of approximately 10%. For the background prediction the statistical and closure systematic uncertainties are considered. The sensitivity is limited mostly by the statistical uncertainty, given the low data yields in the signal regions.

All channels are combined to obtain upper limits at 95% confidence level (CL) on the VBS VVH production cross section as a function of the κ_{2V} coupling modifier. Assuming all other H couplings are equal to their values in the SM, the VBS VVH production is excluded at 95% CL for κ_{2V} outside the observed (expected) range of $0.40 < \kappa_{2V} < 1.60$ ($0.34 < \kappa_{2V} < 1.66$). The results are shown in Fig. 2.

Similarly, the channels are combined to constrain the κ_{2W} and κ_{2Z} parameters, each varied while keeping the other at its SM value, as reported in Fig. 3. The κ_{2W} and κ_{2Z} coupling modifiers are constrained in the (expected) ranges of $0.17 < \kappa_{2W} < 1.84$ ($0.11 < \kappa_{2W} < 1.89$) and $-0.37 < \kappa_{2Z} < 2.38$ ($-0.54 < \kappa_{2Z} < 2.54$), respectively.

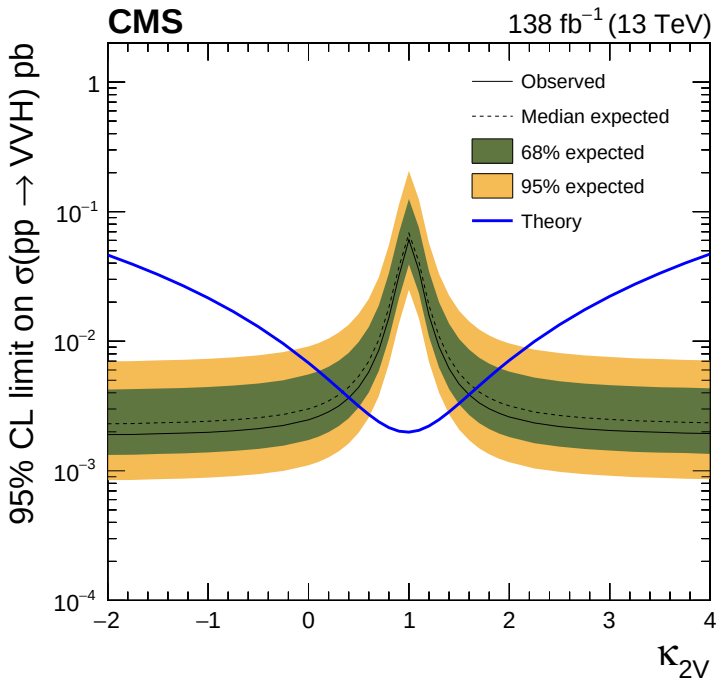

Figure 2: Observed (solid) and expected (dashed) 95% CL constraints on the VBS VVH production cross section as a function of κ_{2V}, with other couplings fixed to their SM values. The intersections with the predicted cross section (blue) indicate the excluded κ_{2V} ranges.

A two-dimensional likelihood scan in the κ_{2W}-κ_{2Z} plane is also performed to derive constraints in that plane. The observed (solid line) and expected (dashed line) exclusion regions corresponding to 1, 2 and 5 standard deviations (σ) are shown in Fig. 4.

Tabulated results are provided in the HEPData record for this analysis [59]. Additional details on the analysis strategies and on the sensitivity achieved in individual channels are provided in the Supplemental Material.

In summary, the first study of VVH production through vector boson scattering is presented, using proton-proton collision data recorded by the CMS experiment at the LHC in 2016–2018, at $\sqrt{s} = 13\,\text{TeV}$, corresponding to an integrated luminosity of $138\,\text{fb}^{-1}$. Selected events are consistent with the presence of two jets originating from VBS and an H decaying into a pair of b quarks, reconstructed as a single large-radius jet. Final states with zero, one, or two charged leptons arising from the decay of two vector bosons are studied. The VBS VVH production is excluded at 95% CL for values of the κ_{2V} coupling modifier outside the observed (expected) range of $0.40 < \kappa_{2V} < 1.60$ ($0.34 < \kappa_{2V} < 1.66$), assuming all other H couplings are equal to their values in the standard model. The results represent one of the best constraints to date on κ_{2V} using CMS data, complementing the results obtained from searches for H pair production, and laying the foundation for future, similar studies. The κ_{2W} and κ_{2Z} coupling modifiers are also constrained independently in the observed (expected) ranges of $0.17 < \kappa_{2W} < 1.84$ ($0.11 < \kappa_{2W} < 1.89$) and $-0.37 < \kappa_{2Z} < 2.38$ ($-0.54 < \kappa_{2Z} < 2.54$), respectively. A two-dimensional scan, determining exclusion regions in the κ_{2W}-κ_{2Z} plane, is also provided, which largely improves on the constraints coming from the CMS search for VHH production.

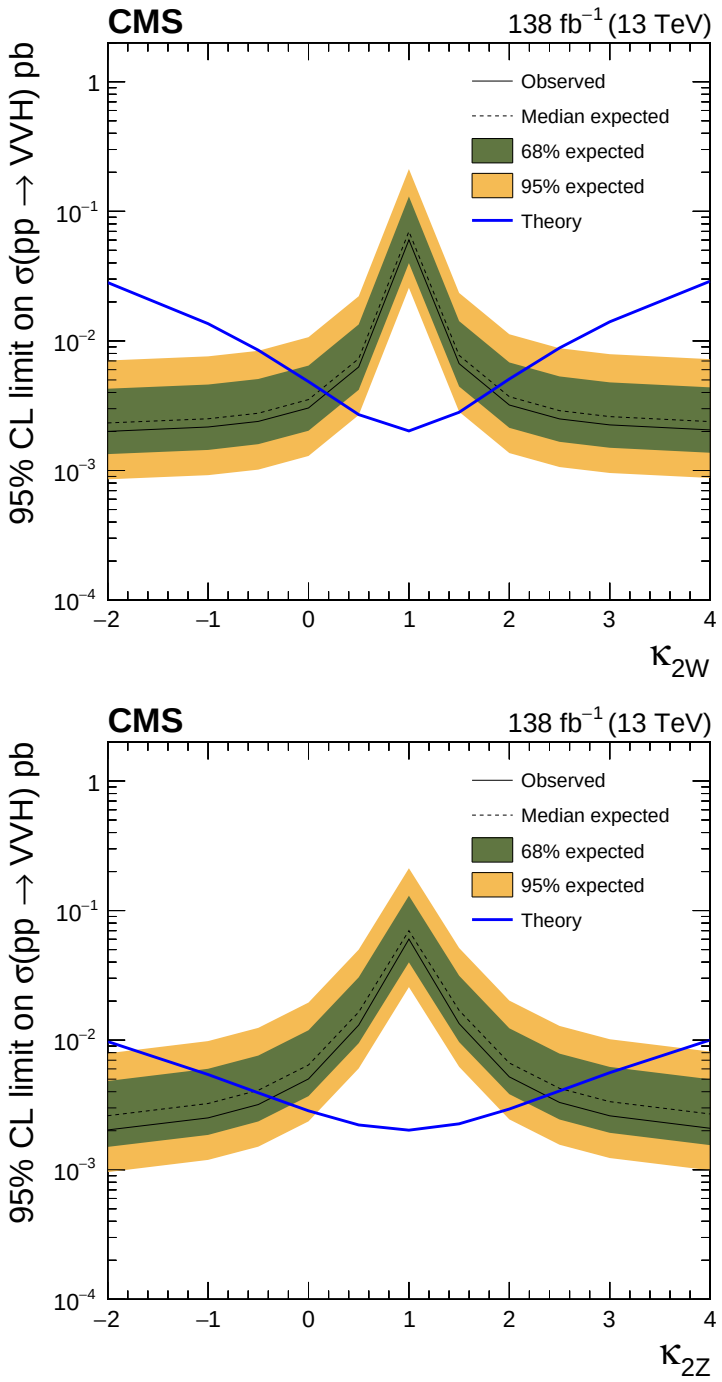

Figure 3: Observed (solid) and expected (dashed) 95% CL constraints on the VBS VVH production cross section as a function of κ_{2W} (upper) and κ_{2Z} (lower). The intersections with the predicted cross section (blue) indicate excluded coupling ranges.

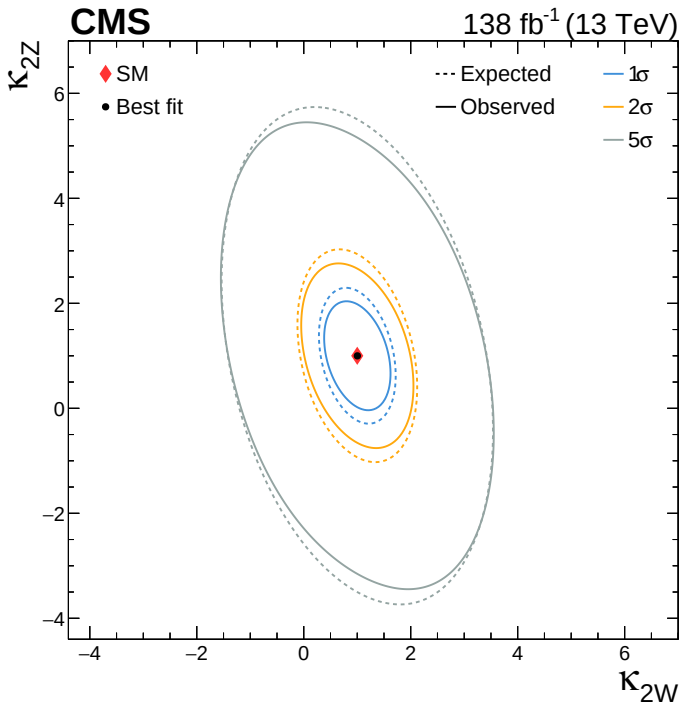

Figure 4: Observed (solid) and expected (dashed) exclusion regions corresponding to 1, 2, and 5 standard deviations (σ), as obtained from a likelihood scan in the two-dimensional κ_{2W}-κ_{2Z} plane.

Acknowledgments

We congratulate our colleagues in the CERN accelerator departments for the excellent performance of the LHC and thank the technical and administrative staffs at CERN and at other CMS institutes for their contributions to the success of the CMS effort. In addition, we gratefully acknowledge the computing centers and personnel of the Worldwide LHC Computing Grid and other centers for delivering so effectively the computing infrastructure essential to our analyses. Finally, we acknowledge the enduring support for the construction and operation of the LHC, the CMS detector, and the supporting computing infrastructure provided by the following funding agencies: SC (Armenia), BMBWF and FWF (Austria); FNRS and FWO (Belgium); CNPq, CAPES, FAPERJ, FAPERGS, and FAPESP (Brazil); MES and BNSF (Bulgaria); CERN; CAS, MoST, and NSFC (China); MINCIENCIAS (Colombia); MSES and CSF (Croatia); RIF (Cyprus); SENESCYT (Ecuador); ERC PRG and PSG, TARISTU24-TK10 and MoER TK202 (Estonia); Academy of Finland, MEC, and HIP (Finland); CEA and CNRS/IN2P3 (France); SRNSF (Georgia); BMFTR, DFG, and HGF (Germany); GSRI (Greece); MATE and NKFIH (Hungary); DAE and DST (India); IPM (Iran); SFI (Ireland); INFN (Italy); MSIT and NRF (Republic of Korea); MES (Latvia); LMTLT (Lithuania); MOE and UM (Malaysia); BUAP, CINVESTAV, CONACYT, LNS, SEP, and UASLP-FAI (Mexico); MOS (Montenegro); MBIE (New Zealand); PAEC (Pakistan); MSHE, NSC, and NAWA (Poland); FCT (Portugal); MESTD (Serbia); MICIU/AEI and PCTI (Spain); MOSTR (Sri Lanka); Swiss Funding Agencies (Switzerland); MST (Taipei); MHESI (Thailand); TUBITAK and TENMAK (Türkiye); NASU (Ukraine); STFC (United Kingdom); DOE and NSF (USA).

References

[1] ATLAS Collaboration, "Observation of a new particle in the search for the standard

model Higgs boson with the ATLAS detector at the LHC", *Phys. Lett. B* **716** (2012) 1, doi:10.1016/j.physletb.2012.08.020, arXiv:1207.7214.

[2] CMS Collaboration, "Observation of a new boson at a mass of 125 GeV with the CMS experiment at the LHC", *Phys. Lett. B* **716** (2012) 30, doi:10.1016/j.physletb.2012.08.021, arXiv:1207.7235.

[3] CMS Collaboration, "Observation of a new boson with mass near 125 GeV in pp collisions at $\sqrt{s} = 7$ and 8 TeV", *JHEP* **06** (2013) 081, doi:10.1007/JHEP06(2013)081, arXiv:1303.4571.

[4] LHC Higgs Cross Section Working Group, S. Heinemeyer et al., "Handbook of LHC Higgs cross sections: 3. Higgs properties", CERN Report CERN-2013-004, 2013. doi:10.5170/CERN-2013-004, arXiv:1307.1347.

[5] LHC Higgs Cross Section Working Group, D. de Florian et al., "Handbook of LHC Higgs cross sections: 4. Deciphering the nature of the Higgs sector", CERN Report CERN-2017-002-M, 2016. doi:10.23731/CYRM-2017-002, arXiv:1610.07922.

[6] CMS Collaboration, "Combination of searches for nonresonant Higgs boson pair production in proton-proton collisions at $\sqrt{s}$ = 13 TeV", 2025. arXiv:2510.07527. Submitted to Journal of Physics G.

[7] ATLAS Collaboration, "Combination of searches for Higgs boson pair production in pp collisions at $\sqrt{s}$ = 13 TeV with the ATLAS detector", *Phys. Rev. Lett.* **133** (2024) 101801, doi:10.1103/PhysRevLett.133.101801, arXiv:2406.09971.

[8] J. Alwall et al., "The automated computation of tree-level and next-to-leading order differential cross sections, and their matching to parton shower simulations", *JHEP* **07** (2014) 079, doi:10.1007/JHEP07(2014)079, arXiv:1405.0301.

[9] CMS Collaboration, "Improved results on Higgs boson pair production in the 4b final state", 2026. arXiv:2604.27044. Submitted to Phys. Rev. D.

[10] CMS Collaboration, "Search for Higgs boson pair production with one associated vector boson in proton-proton collisions at $\sqrt{s} = 13$ TeV", *JHEP* **10** (2024) 061, doi:10.1007/JHEP10(2024)061, arXiv:2404.08462.

[11] CMS Collaboration, "The CMS experiment at the CERN LHC", *JINST* **3** (2008) S08004, doi:10.1088/1748-0221/3/08/S08004.

[12] CMS Collaboration, "Development of the CMS detector for the CERN LHC Run 3", *JINST* **19** (2024) P05064, doi:10.1088/1748-0221/19/05/P05064, arXiv:2309.05466.

[13] CMS Collaboration, "Performance of the CMS Level-1 trigger in proton-proton collisions at $\sqrt{s} = 13$ TeV", *JINST* **15** (2020) P10017, doi:10.1088/1748-0221/15/10/P10017, arXiv:2006.10165.

[14] CMS Collaboration, "The CMS trigger system", *JINST* **12** (2017) P01020, doi:10.1088/1748-0221/12/01/P01020, arXiv:1609.02366.

[15] CMS Collaboration, "Performance of the CMS high-level trigger during LHC Run 2", *JINST* **19** (2024) P11021, doi:10.1088/1748-0221/19/11/P11021, arXiv:2410.17038.

[16] CMS Collaboration, "Electron and photon reconstruction and identification with the CMS experiment at the CERN LHC", *JINST* **16** (2021) P05014, doi:10.1088/1748-0221/16/05/P05014, arXiv:2012.06888.

[17] CMS Collaboration, "Performance of the CMS muon detector and muon reconstruction with proton-proton collisions at $\sqrt{s} = 13$ TeV", *JINST* **13** (2018) P06015, doi:10.1088/1748-0221/13/06/P06015, arXiv:1804.04528.

[18] CMS Collaboration, "Description and performance of track and primary-vertex reconstruction with the CMS tracker", *JINST* **9** (2014) P10009, doi:10.1088/1748-0221/9/10/P10009, arXiv:1405.6569.

[19] CMS Collaboration, "Particle-flow reconstruction and global event description with the CMS detector", *JINST* **12** (2017) P10003, doi:10.1088/1748-0221/12/10/P10003, arXiv:1706.04965.

[20] CMS Collaboration, "Performance of reconstruction and identification of τ leptons decaying to hadrons and ν_τ in pp collisions at $\sqrt{s} = 13$ TeV", *JINST* **13** (2018) P10005, doi:10.1088/1748-0221/13/10/P10005, arXiv:1809.02816.

[21] CMS Collaboration, "Jet energy scale and resolution in the CMS experiment in pp collisions at 8 TeV", *JINST* **12** (2017) P02014, doi:10.1088/1748-0221/12/02/P02014, arXiv:1607.03663.

[22] CMS Collaboration, "Performance of missing transverse momentum reconstruction in proton-proton collisions at $\sqrt{s} = 13$ TeV using the CMS detector", *JINST* **14** (2019) P07004, doi:10.1088/1748-0221/14/07/P07004, arXiv:1903.06078.

[23] CMS Collaboration, "Technical proposal for the Phase-II upgrade of the Compact Muon Solenoid", CMS Technical Proposal CERN-LHCC-2015-010, CMS-TDR-15-02, 2015.

[24] CMS Collaboration, "ECAL 2016 refined calibration and Run2 summary plots", CMS Detector Performance Summary CMS-DP-2020-021, 2020.

[25] CMS Collaboration, "Measurement of the Higgs boson production rate in association with top quarks in final states with electrons, muons, and hadronically decaying tau leptons at $\sqrt{s} = 13$ TeV", *Eur. Phys. J. C* **81** (2021) 378, doi:10.1140/epjc/s10052-021-09014-x, arXiv:2011.03652.

[26] CMS Collaboration, "Identification of hadronic tau lepton decays using a deep neural network", *JINST* **17** (2022) P07023, doi:10.1088/1748-0221/17/07/P07023, arXiv:2201.08458.

[27] M. Cacciari, G. P. Salam, and G. Soyez, "The anti-k_T jet clustering algorithm", *JHEP* **04** (2008) 063, doi:10.1088/1126-6708/2008/04/063, arXiv:0802.1189.

[28] M. Cacciari, G. P. Salam, and G. Soyez, "FastJet user manual", *Eur. Phys. J. C* **72** (2012) 1896, doi:10.1140/epjc/s10052-012-1896-2, arXiv:1111.6097.

[29] CMS Collaboration, "Pileup mitigation at CMS in 13 TeV data", *JINST* **15** (2020) P09018, doi:10.1088/1748-0221/15/09/P09018, arXiv:2003.00503.

[30] D. Bertolini, P. Harris, M. Low, and N. Tran, "Pileup per particle identification", *JHEP* **10** (2014) 059, doi:10.1007/JHEP10(2014)059, arXiv:1407.6013.

[31] H. Qu and L. Gouskos, "ParticleNet: Jet tagging via particle clouds", *Phys. Rev. D* **101** (2020) 056019, doi:10.1103/PhysRevD.101.056019, arXiv:1902.08570.

[32] A. J. Larkoski, S. Marzani, G. Soyez, and J. Thaler, "Soft drop", *JHEP* **05** (2014) 146, doi:10.1007/JHEP05(2014)146, arXiv:1402.2657.

[33] M. Dasgupta, A. Fregoso, S. Marzani, and G. P. Salam, "Towards an understanding of jet substructure", *JHEP* **09** (2013) 029, doi:10.1007/JHEP09(2013)029, arXiv:1307.0007.

[34] J. M. Butterworth, A. R. Davison, M. Rubin, and G. P. Salam, "Jet substructure as a new Higgs search channel at the LHC", *Phys. Rev. Lett.* **100** (2008) 242001, doi:10.1103/PhysRevLett.100.242001, arXiv:0802.2470.

[35] CMS Collaboration, "Identification of heavy-flavour jets with the CMS detector in pp collisions at 13 TeV", *JINST* **13** (2018) P05011, doi:10.1088/1748-0221/13/05/P05011, arXiv:1712.07158.

[36] E. Bols et al., "Jet flavour classification using DeepJet", *JINST* **15** (2020) P12012, doi:10.1088/1748-0221/15/12/P12012, arXiv:2008.10519.

[37] CMS Collaboration, "Performance of the DeepJet b tagging algorithm using 41.9 fb^{-1} of data from proton-proton collisions at 13 TeV with Phase 1 CMS detector", CMS Detector Performance Summary CMS-DP-2018-058, 2018.

[38] T. Sjöstrand et al., "An introduction to PYTHIA 8.2", *Comput. Phys. Commun.* **191** (2015) 159, doi:10.1016/j.cpc.2015.01.024, arXiv:1410.3012.

[39] B. Cabouat and T. Sjöstrand, "Some dipole shower studies", *Eur. Phys. J. C* **78** (2018) 226, doi:10.1140/epjc/s10052-018-5645-z, arXiv:1710.00391.

[40] O. Mattelaer, "On the maximal use of Monte Carlo samples: re-weighting events at NLO accuracy", *Eur. Phys. J. C* **76** (2016) 674, doi:10.1140/epjc/s10052-016-4533-7, arXiv:1607.00763.

[41] S. Frixione, P. Nason, and G. Ridolfi, "A positive-weight next-to-leading-order Monte Carlo for heavy flavour hadroproduction", *JHEP* **09** (2007) 126, doi:10.1088/1126-6708/2007/09/126, arXiv:0707.3088.

[42] P. Nason, "A new method for combining NLO QCD with shower Monte Carlo algorithms", *JHEP* **11** (2004) 040, doi:10.1088/1126-6708/2004/11/040, arXiv:hep-ph/0409146.

[43] S. Frixione, P. Nason, and C. Oleari, "Matching NLO QCD computations with parton shower simulations: the POWHEG method", *JHEP* **11** (2007) 070, doi:10.1088/1126-6708/2007/11/070, arXiv:0709.2092.

[44] S. Alioli, P. Nason, C. Oleari, and E. Re, "A general framework for implementing NLO calculations in shower Monte Carlo programs: the POWHEG BOX", *JHEP* **06** (2010) 043, doi:10.1007/JHEP06(2010)043, arXiv:1002.2581.

[45] J. Alwall et al., "Comparative study of various algorithms for the merging of parton showers and matrix elements in hadronic collisions", *Eur. Phys. J. C* **53** (2008) 473, doi:10.1140/epjc/s10052-007-0490-5, arXiv:0706.2569.

[46] CMS Collaboration, "Extraction and validation of a new set of CMS PYTHIA8 tunes from underlying-event measurements", *Eur. Phys. J. C* **80** (2020) 4, doi:10.1140/epjc/s10052-019-7499-4, arXiv:1903.12179.

[47] NNPDF Collaboration, "Parton distributions for the LHC Run II", *JHEP* **04** (2015) 040, doi:10.1007/JHEP04(2015)040, arXiv:1410.8849.

[48] NNPDF Collaboration, "Parton distributions from high-precision collider data", *Eur. Phys. J. C* **77** (2017) 663, doi:10.1140/epjc/s10052-017-5199-5, arXiv:1706.00428.

[49] GEANT4 Collaboration, "GEANT4—a simulation toolkit", *Nucl. Instrum. Meth. A* **506** (2003) 250, doi:10.1016/S0168-9002(03)01368-8.

[50] CDF Collaboration, "Measurement of $\sigma B(W \to e\nu)$ and $\sigma B(Z^0 \to e^+e^-)$ in $\bar{p}p$ collisions at $\sqrt{s} = 1800$ GeV", *Phys. Rev. D* **44** (1991) 29, doi:10.1103/PhysRevD.44.29.

[51] G. Kasieczka, B. Nachman, M. D. Schwartz, and D. Shih, "Automating the ABCD method with machine learning", *Phys. Rev. D* **103** (2021) 035021, doi:10.1103/PhysRevD.103.035021, arXiv:2007.14400.

[52] Particle Data Group, S. Navas et al., "Review of particle physics", *Phys. Rev. D* **110** (2024) 030001, doi:10.1103/PhysRevD.110.030001.

[53] CMS Collaboration, "The CMS statistical analysis and combination tool: Combine", *Comput. Softw. Big Sci.* **8** (2024) 19, doi:10.1007/s41781-024-00121-4, arXiv:2404.06614.

[54] W. Verkerke and D. Kirkby, "The ROOFIT toolkit for data modeling", in *Proc. 13th International Conference on Computing in High Energy and Nuclear Physics (CHEP 2003): La Jolla CA, United States, March 24–28, 2003*. 2003. arXiv:physics/0306116. [eConf C0303241 (2003) MOLT007].

[55] L. Moneta et al., "The ROOSTATS project", in *Proc. 13th International Workshop on Advanced Computing and Analysis Techniques in Physics Research (ACAT 2010): Jaipur, India, February 22–27, 2010*. 2010. arXiv:1009.1003. [PoS (ACAT2010) 057]. doi:10.22323/1.093.0057.

[56] CMS Collaboration, "Precision luminosity measurement in proton-proton collisions at $\sqrt{s} = 13$ TeV in 2015 and 2016 at CMS", *Eur. Phys. J. C* **81** (2021) 800, doi:10.1140/epjc/s10052-021-09538-2, arXiv:2104.01927.

[57] CMS Collaboration, "CMS luminosity measurement for the 2017 data-taking period at $\sqrt{s} = 13$ TeV", CMS Physics Analysis Summary CMS-PAS-LUM-17-004, 2018.

[58] CMS Collaboration, "CMS luminosity measurement for the 2018 data-taking period at $\sqrt{s} = 13$ TeV", CMS Physics Analysis Summary CMS-PAS-LUM-18-002, 2019.

[59] HEPData record for this analysis, 2026. doi:10.17182/hepdata.161535.

[60] "Supplemental Material: validation studies of the neural network classifiers and background-estimation method used in the analysis, together with per-channel results for the upper limits on the coupling modifiers". [URL will be inserted by publisher].

A End Matter

A.1 Event selection

This section details the event selections used in each channel before multivariate analyses are performed. In the all-hadronic channels, events of interest are collected using triggers based on H_T, with thresholds of 800 or 900 GeV for 2016, and 1050 GeV for 2017 and 2018. Events must contain at least two AK8 jets with $p_T > 300$ GeV, and $p_T > 550$ GeV for the leading one to ensure full trigger efficiency. Two categories are defined to distinguish fully and semi-boosted events. In the fully boosted channel, the $H \to b\bar{b}$ candidate is selected as the AK8 jet with the highest $X \to b\bar{b}$ PARTICLENET score (> 0.5), and the vector boson candidates are selected as the two highest p_T remaining AK8 jets with $X \to qq$ scores > 0.3. In the semi-boosted channel, exactly two AK8 jets are required. The $H \to b\bar{b}$ candidate is selected as the AK8 jet with the highest $X \to b\bar{b}$ score (> 0.8). One of the two vector bosons is reconstructed as the other AK8 jet in the event, requiring an $X \to qq$ minimum score of 0.637, 0.579, and 0.59 for 2016, 2017, and 2018 data taking, respectively. The second vector boson is reconstructed from two AK4 jets ($p_T > 20$ GeV, $|\eta| < 2.5$) chosen as the closest pair in ΔR. Two AK4 VBS jet candidates are also required. In the case of multiple pairs, the one with the largest $|\Delta\eta_{jj}|$ is selected as the VBS jet pair. The selection criteria for the all-hadronic fully boosted and semi-boosted channels are summarized in Tables 1 and 2, respectively.

Table 1: Selection criteria used in the all-hadronic fully boosted channel. If selection criteria differ across years, they are quoted as "2016/2017/2018".

Selection	Description
Trigger	$H_T > 800$ or 900/1050/1050 GeV
Loose lepton count	$=0$
Tight lepton count	$=0$
AK8 jet threshold	$p_T > 300$ GeV
AK8 jet count	>2
Leading AK8 jet	$p_T > 550$ GeV
$H \to b\bar{b}$ candidate	max $X \to b\bar{b}$ score AK8 jet
	$X \to b\bar{b}$ score > 0.5
$V \to qq$ candidates	p_T-leading AK8 jets
	$X \to qq$ score > 0.3
AK4 jet count for VBS	≥ 2
VBS jet candidates	max $\lvert\Delta\eta_{jj}\rvert$

In the single-lepton channel, single-lepton triggers require isolated leptons with $p_T > 24$ (27) GeV for muons in 2016 and 2018 (2017), and $p_T > 27$ (32) GeV for electrons in 2016 (2017–2018). Events must contain exactly one tight lepton with $p_T > 40$ GeV and no additional loose leptons. Two AK8 jets with $p_T > 250$ GeV are required. The $H \to b\bar{b}$ candidate is reconstructed as the AK8 jet with the highest $X \to b\bar{b}$ PARTICLENET score, while the hadronic vector boson candidate is the remaining AK8 jet with the highest $X \to qq$ score. The VBS jets are chosen as the highest-momentum jets in opposite η regions; if this criterion fails, the two highest-momentum jets are selected. Events with AK4 jets passing the tight DEEPJET working point are rejected. Jets passing the loose working point are used to define $m_{\ell b}$, the minimum invariant mass of the lepton and any b jet, used in the multivariate analysis to suppress the $t\bar{t}$ background. Furthermore, a selection is applied on $S_T > 1000$ GeV. The selection criteria for the single-lepton channel are summarized in Table 3.

In the dilepton channels, single-lepton triggers are used for OS WW events. These are used

Table 2: Selection criteria used in the all-hadronic semi-boosted channel. If the selection criteria differ across years, they are quoted as "2016/2017/2018".

Selection	Description
Trigger	$H_T > 800$ or 900/1050/1050 GeV
Loose lepton count	$=0$
Tight lepton count	$=0$
AK8 jet threshold	$p_T > 300$ GeV
AK8 jet count	$=2$
Leading AK8 jet	$p_T > 550$ GeV
$H \to b\bar{b}$ candidate	max $X \to b\bar{b}$ score AK8 jet
	$X \to b\bar{b}$ score > 0.8
Boosted $V \to qq$ candidate	other AK8 jet
	$X \to qq$ score $> 0.637/0.579/0.59$
AK4 jet for $V \to qq$ criteria	$p_T > 20$ GeV, $\lvert\eta\rvert < 2.5$
AK4 jet for $V \to qq$ count	≥ 2
Resolved $V \to qq$ candidate	min ΔR
AK4 jet count for VBS	≥ 2
VBS jet candidates	max $\lvert\Delta\eta_{jj}\rvert$

Table 3: Selection criteria used in the single-lepton channel. If the selection criteria differ across years, they are quoted as "2016/2017/2018".

Selection	Description
Trigger	Single-muon $p_T > 24/27/24$ GeV
	Single-electron $p_T > 27/32/32$ GeV
Sign and flavor of leptons	$e^{\pm}$, $\mu^{\pm}$
Loose lepton count	$=1$
Tight lepton count	$=1$
Tight lepton p_T	$p_T > 40$ GeV
AK8 jet threshold	$p_T > 250$ GeV
AK8 jet count	≥ 2
$H \to b\bar{b}$ candidate	max $X \to b\bar{b}$ score AK8 jet
$V \to qq$ candidate	max $X \to qq$ score AK8 jet
AK4 jet count for VBS	≥ 2
VBS jet candidates	max momentum, opposite η sign
AK4 jet for b tagging criteria	$p_T > 20$ GeV, $\lvert\eta\rvert < 2.5$
Tight b tagged jet count	$=0$
Event kinematics	$S_T > 1000$ GeV

in combination with dilepton triggers for OS Z events, with p_T thresholds of 17 and 8 GeV for muons, and 23 and 12 GeV for electrons. In OS WW events, electrons must have $p_T > 29\,(34)$ GeV in 2016 (2017–2018), and muons $p_T > 26\,(29)$ GeV in 2016 and 2018 (2017). The two leptons must be oppositely charged and separated with $\Delta R > 0.5$. A Z boson mass veto excludes events with $86 < m_{\ell\ell} < 96$ GeV. The H candidate is selected as the AK8 jet with the highest $X \to b\bar{b}$ PARTICLENET score, $p_T > 250$ GeV, and $70 < m_{PN} < 160$ GeV. Events with AK4 jets passing the DEEPJET medium working point are rejected, and the two jets with the largest $\lvert\Delta\eta_{jj}\rvert$ are selected as VBS jet candidates. Events must have $p_T^{miss} > 100$ GeV and $S_T > 500$ GeV. In OS Z events, the leading muons (electrons) must have $p_T > 19\,(25)$ GeV, and the subleading $p_T > 12\,(18)$ GeV. The leptons must be oppositely charged, with $86 <$

$m_{\ell\ell} < 96\,\text{GeV}$. The $\text{H} \to \text{b}\overline{\text{b}}$ candidate is selected as the AK8 jet with $p_\text{T} > 250\,\text{GeV}$ and highest $X \to \text{b}\overline{\text{b}}$ score (>0.2), while the hadronically decaying vector boson candidate is the AK8 jet with $p_\text{T} > 200\,\text{GeV}$ and highest $X \to \text{qq}$ score (>0.6). The invariant mass M_VVH of the $\text{H} \to \text{b}\overline{\text{b}}$ candidate, the hadronically decaying vector boson candidate and the lepton pair, and S_T must both exceed 500 GeV. The VBS jet pair is chosen based on the largest $|\Delta\eta_{\text{jj}}|$, with the minimum requirements of $m_{\text{jj}} > 200\,\text{GeV}$ and $|\Delta\eta_{\text{jj}}| > 2$. Events with AK4 jets passing the DEEPJET medium working point are rejected. The selection criteria used for OS dilepton events are summarized in Tables 4 and 5 for the OS WW and OS Z channels, respectively.

Table 4: Selection criteria in used the OS WW dilepton channel. If the selection criteria differ across years, they are quoted as "2016/2017/2018".

Selection	Description
Trigger	Single-muon $p_\text{T} > 24/27/24\,\text{GeV}$
	Single-electron $p_\text{T} > 27/32/32\,\text{GeV}$
Sign and flavor of leptons	e^+e^-, $\mu^+\mu^-$, $\mu^\pm\text{e}^\mp$
Loose lepton count	$=2$
Tight lepton count	$=2$
Lepton p_T	$p_\text{T} > 26/29/26\,\text{GeV}$ (muons)
	$p_\text{T} > 29/34/34\,\text{GeV}$ (electrons)
Tight lepton separation	$\Delta R > 0.5$
Z veto	$m_{\ell\ell} < 86$ or $> 96\,\text{GeV}$
AK8 jet threshold	$p_\text{T} > 250\,\text{GeV}$
AK8 jet count	≥ 1
$\text{H} \to \text{b}\overline{\text{b}}$ candidate	max $X \to \text{b}\overline{\text{b}}$ score AK8 jet
	$70 < m_\text{PN} < 160\,\text{GeV}$
AK4 jet count for VBS	≥ 2
VBS jet candidates	max $\lvert\Delta\eta_{\text{jj}}\rvert$
AK4 jet for b tagging criteria	$p_\text{T} > 20\,\text{GeV}$, $\lvert\eta\rvert < 2.5$
Medium b tagged jet count	$=0$
Missing transverse momentum	$p_\text{T}^\text{miss} > 100\,\text{GeV}$
Event kinematics	$\text{S}_\text{T} > 500\,\text{GeV}$

The SS dilepton channel also uses mixed muon-electron triggers, requiring a muon (electron) with $p_\text{T} > 23\,(12)\,\text{GeV}$ and an electron (muon) with $p_\text{T} > 23\,(8)\,\text{GeV}$, besides the single and dilepton triggers used in the OS dilepton channel. Exactly two tight leptons are required, with no additional loose leptons. Both leptons are required to have $p_\text{T} > 30\,\text{GeV}$, allowing at most one hadronically decaying τ lepton. At least one AK8 jet with $p_\text{T} > 250\,\text{GeV}$ and two VBS jet candidates failing the medium DEEPJET working point are required. If more than two VBS jet candidates are found, the same selection as in the single-lepton channel is applied. To suppress events that are not consistent with VBS production, $m_{\text{jj}} > 100\,\text{GeV}$ is required. The signal region is defined by $m_{\text{jj}} > 500\,\text{GeV}$, $|\Delta\eta_{\text{jj}}| > 3$, and $X \to \text{b}\overline{\text{b}}$ score > 0.9. A control region includes events with $m_{\text{jj}} > 100\,\text{GeV}$ that fail the m_{jj} or $\Delta\eta_{\text{jj}}$ selections with respect to the signal region, with no requirement on the $X \to \text{b}\overline{\text{b}}$ score of the selected AK8 jet. The selection criteria for the SS dilepton channel are summarized in Table 6.

A.2 Signal region definition

After the event selection, a multivariate analysis is performed in all channels. In the all-hadronic, single-lepton and OS dilepton channels, an "ABCD" method [50] is used: the signal

Table 5: Selection criteria used in the OS Z dilepton channel. If the selection criteria differ across years, they are quoted as "2016/2017/2018".

Selection	Description
Trigger	Single-muon $p_T > 24/27/24$ GeV
	Single-electron $p_T > 27/32/32$ GeV
	Dimuon $p_T > 17\,(8)$ GeV
	Dielectron $p_T > 23\,(12)$ GeV
Sign and flavor of leptons	e^+e^-, $\mu^+\mu^-$
Loose lepton count	=2
Tight lepton count	=2
Leading lepton p_T	$p_T > 19\,(25)$ GeV muon (electron)
Subleading lepton p_T	$p_T > 12\,(18)$ GeV muon (electron)
Z window	$86 < m_{\ell\ell} < 96$ GeV
AK8 jet threshold	$p_T > 250/200$ GeV
AK8 jet count	≥2
$H \to b\bar{b}$ candidate	max $X \to b\bar{b}$ score AK8 jet
	$X \to b\bar{b}$ score >0.2
Boosted $V \to qq$ candidate	Other AK8 jet
	$X \to qq$ score >0.6
AK4 jet count for VBS	≥2
VBS jet candidates	max $\lvert\Delta\eta_{jj}\rvert$
	$m_{jj} > 200$ GeV, $\lvert\Delta\eta_{jj}\rvert > 2$
AK4 jet for b tagging criteria	$p_T > 20$ GeV, $\lvert\eta\rvert < 2.5$
Medium b tagged jet count	=0
Event kinematics	$S_T > 500$ GeV
	$M_{VVH} > 500$ GeV

region, or region A, is defined alongside orthogonal control regions B, C, and D, used to predict the background in region A from data. The selections used in each channel to define the signal region, or region A, are summarized in Table 7. The "AC axis" selection, relying on the properties of the VVH system, is inverted to define the region C; the "AB axis" selection, using the properties of the VBS jets, is inverted to define the region B; both are inverted to define the region D. Additional selections, depending on the channel, are applied after the training of the discriminators to further improve the sensitivity of the search, and are common to the regions A, B, C and D. These selections are applied only after the training in order to preserve the statistical power of the simulated samples at training time. They are limited to the PARTICLENET $X \to b\bar{b}$ and $X \to qq$ scores, which are largely independent of the global event kinematic properties.

In the SS dilepton channel, a BDT is also trained to discriminate signal from background, and the signal region is divided into three bins according to the BDT output score ($[0, 0.1]$, $[0.1, 0.25]$, $[0.25, 1]$).

A.3 Event yields

Table 8 shows the data yields in the regions A, B, C and D of the all-hadronic, single-lepton, and OS dilepton channels, alongside the predicted background with its uncertainties, and the signal expected in region A for the $\kappa_{2V} = 2$ and SM benchmark scenarios. The background is predicted to be small in region A for all channels, except for the all-hadronic semi-boosted channel, where the contribution of the QCD multijet background is larger. Systematic uncer-

Table 6: Selection criteria used in the SS dilepton channel. If the selection criteria differ across years, they are quoted as "2016/2017/2018".

Selection	Description
Trigger	Single-muon $p_T > 24/27/24\,\text{GeV}$
	Single-electron $p_T > 27/32/32\,\text{GeV}$
	Dimuon $p_T > 17\,(8)\,\text{GeV}$
	Dielectron $p_T > 23\,(12)\,\text{GeV}$
	Electron (muon) $p_T > 23\,(8)\,\text{GeV}$
	Muon (electron) $p_T > 23\,(12)\,\text{GeV}$
Sign and flavor of leptons	$e^{\pm}e^{\pm}$, $\mu^{\pm}\mu^{\pm}$, $e^{\pm}\mu^{\pm}$, $\mu^{\pm}\tau^{\pm}$, $e^{\pm}\tau^{\pm}$
Loose lepton count	$= 2$
Tight lepton count	$= 2$
Lepton p_T	$p_T > 30\,\text{GeV}$
AK8 jet threshold	$p_T > 250\,\text{GeV}$
AK8 jet count	≥ 1
$H \to b\bar{b}$ candidate	max $X \to b\bar{b}$ score AK8 jet
Medium b tagged jet count	$= 0$
AK4 jet count for VBS	≥ 2
VBS jet candidates	max momentum jets, opposite η sign
	$m_{jj} > 100\,\text{GeV}$
Signal region	$m_{jj} > 500\,\text{GeV}$, $\lvert\Delta\eta_{jj}\rvert > 3$,
	$X \to b\bar{b}$ score > 0.9 for $H \to b\bar{b}$ candidate
Control region	$m_{jj} > 100\,\text{GeV}$,
	with $m_{jj} < 500\,\text{GeV}$ or $\lvert\Delta\eta_{jj}\rvert < 3$

tainties in the background predictions are derived from closure tests in data. The systematic uncertainties in the signal yields correspond to the sum in quadrature of all the experimental and theoretical uncertainties. The statistical unceratainties arise from the limited size of the simulated samples for signal, and from the amount of data in regions B, C and D for the background.

Table 9 shows the data yields and the predicted background in the signal (SR) and control regions (CR) of the same-sign dilepton channel for the $\ell\ell$, where $\ell = e, \mu$, and the $\ell\tau$ categories, alongside with the expected yields for the benchmark SM signal. The total uncertainty in the background is shown, which accounts for both statistical and systematic sources.

Table 7: Summary of the selections used to define the signal region, or region A, in the all-hadronic, single-lepton, and OS dilepton channels. The selections on the "AB axis" and "AC axis" are inverted to define the regions B, C and D. Additional selections on the $X \to b\bar{b}$ and $X \to qq$ scores are applied after the training to further improve the sensitivity of the search. For the all-hadronic fully boosted channel, the selections on the $X \to qq$ score are applied on the p_T-leading/subleading vector boson candidates.

	All-hadronic		Single-lepton	Dilepton	
	fully boosted	semi-boosted		OS W W	OS Z
AC axis (VVH)	DNN $>$ 0.97	DNN $>$ 0.8	DNN $>$ 0.9	BDT $>$ 0.85	BDT $>$ 0.85
AB axis (VBS)	$\lvert\Delta\eta_{jj}\rvert > 5$	$\lvert\Delta\eta_{jj}\rvert > 6$ $m_{jj} > 1300\,\text{GeV}$	BDT $>$ 0.82	$\lvert\Delta\eta_{jj}\rvert > 4.9$ $m_{jj} > 760\,\text{GeV}$	$\lvert\Delta\eta_{jj}\rvert > 4$ $m_{jj} > 750\,\text{GeV}$
$X \to b\bar{b}$ score	$>$0.8	—	$>$0.5	$>$0.7	—
$X \to qq$ score	$>$0.8/0.7	—	$>$0.7	—	—

Table 8: Data yields in regions B, C and D, used to estimate the background in region A, along with data, predicted background, and expected signal in region A. Signal yields are shown for the SM and $\kappa_{2V} = 2$ benchmarks.

	All-hadronic		Single-lepton	Dilepton	
	fully boosted	semi-boosted		OS W W	OS Z
B data	1	410	3	2	1
C data	73	399	61	10	5
D data	654	15 974	1039	179	17
A data	0	7	0	0	0
A prediction	$0.11^{+0.26}_{-0.09}$ (stat) $\pm$0.03 (syst)	$10.24^{+0.78}_{-0.72}$ (stat) $\pm$1.95 (syst)	$0.18^{+0.18}_{-0.10}$ (stat) $\pm$0.06 (syst)	$0.11^{+0.18}_{-0.08}$ (stat) $\pm$0.02 (syst)	$0.29^{+0.91}_{-0.25}$ (stat) $\pm$0.21 (syst)
A signal ($\kappa_{2V} = 2$)	3.30 ± 0.02 (stat) $\pm$1.01 (syst)	1.06 ± 0.01 (stat) $\pm$0.36 (syst)	2.79 ± 0.02 (stat) $\pm$0.84 (syst)	0.31 ± 0.01 (stat) $\pm$0.10 (syst)	$0.22 \pm (< 0.01)$ (stat) $\pm$0.07 (syst)
A signal (SM)	0.04 ± 0.01	$0.01 \pm (<0.01)$	0.04 ± 0.02	$0.01 \pm (<0.01)$	$(<0.01) \pm (<0.01)$

Table 9: Data yields, predicted background and expected signal in signal (SR) and control regions (CR) of the same-sign dilepton channel.

	Same-sign dilepton			
	$\ell\ell$ SR	$\ell\ell$ CR	$\ell\tau$ SR	$\ell\tau$ CR
Data	4	39	3	49
Background	1.90 ± 0.33	27.90 ± 3.67	3.46 ± 0.55	50.52 ± 8.09
Signal (SM)	$0.01 \pm (< 0.01)$	$(<0.01) \pm (< 0.01)$	$(<0.01) \pm (< 0.01)$	$(<0.01) \pm (<0.01)$

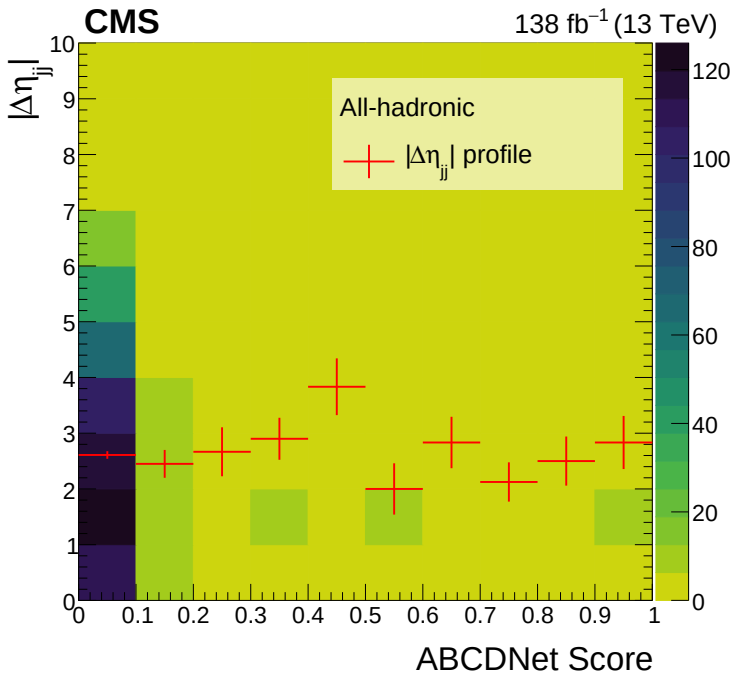

Figure B.1: Two-dimensional distribution of the DNN output and the $|\Delta\eta_{jj}|$ in the all-hadronic channel, as obtained in data. These are the axes used in this channel to define the ABCD samples. A profile histogram is overlaid to better depict the statistical independence of the two variables.

B Supplemental Material

B.1 Neural network event classifiers

The results presented in this paper exploit deep neural network (DNN) classifiers to select events and define signal and control regions. Below we present additional studies on these DNNs and on the definition of the "ABCD" samples that are used to estimate the backgrounds in the all-hadronic, single-lepton and OS dilepton channels of the analysis.

Figures B.1 and B.2 (Figs. B.3 and B.4) demonstrate the statistical independence of the variables used to define the ABCD axes in the all-hadronic (single-lepton) channel, in data and in simulated events, respectively.

Figures B.5 and B.6 (figures B.7 and B.8) show the distributions of the DNN output in the regions B and D and in the regions A and C of the all-hadronic (single-lepton) channel, respectively.

B.2 Analysis sensitivity: additional studies

The results presented in the paper are a combination of the six analysis channels. Below we present results obtained in individual channels, including comparisons to those arising from their combination.

Figures B.10 and B.11 show the 95% CL expected and observed upper limits on the VBS VVH production cross section as a function of the κ_{2V} coupling modifier for each analysis channel. The combined 95% CL upper limits are also shown.

Figures B.10 and B.11 show the 95% CL upper limits on the VBS VVH production cross section

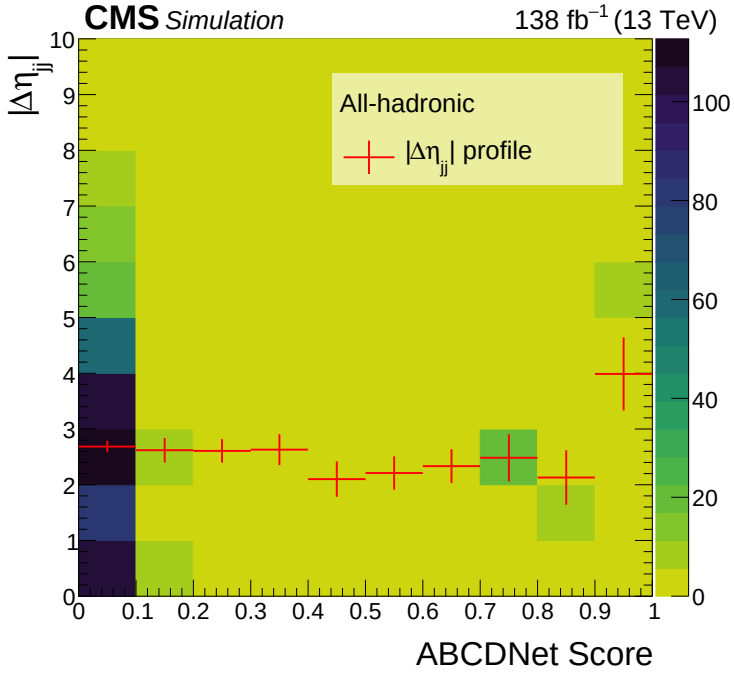

Figure B.2: Two-dimensional distribution of the DNN output and the $|\Delta\eta_{jj}|$ in the all-hadronic channel, as obtained in background simulated events. These are the axes used in this channel to define the ABCD samples. A profile histogram is overlaid to better depict the statistical independence of the two variables.

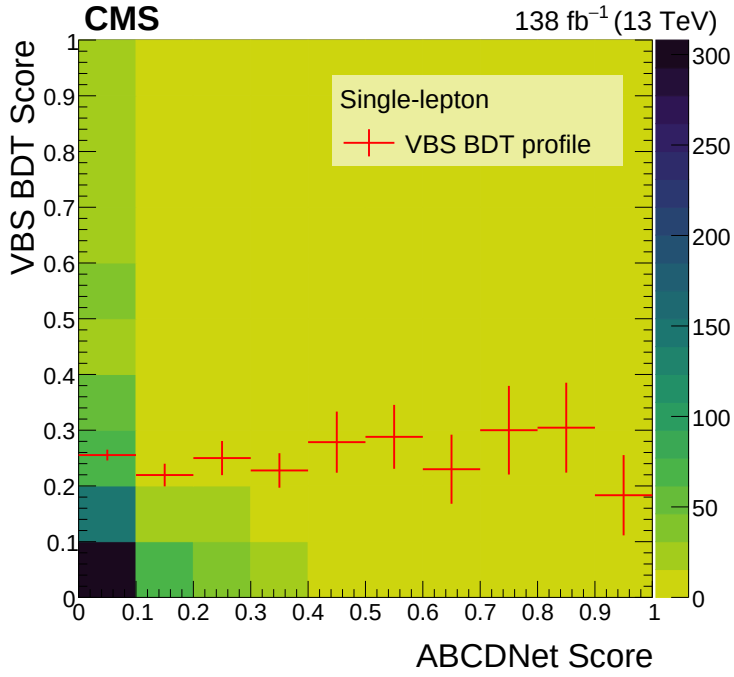

Figure B.3: Two-dimensional distribution of the DNN output and the VBS BDT output in the single-lepton channel, as obtained in data. These are the axes used in this channel to define the ABCD samples. A profile histogram is overlaid to better depict the statistical independence of the two variables.

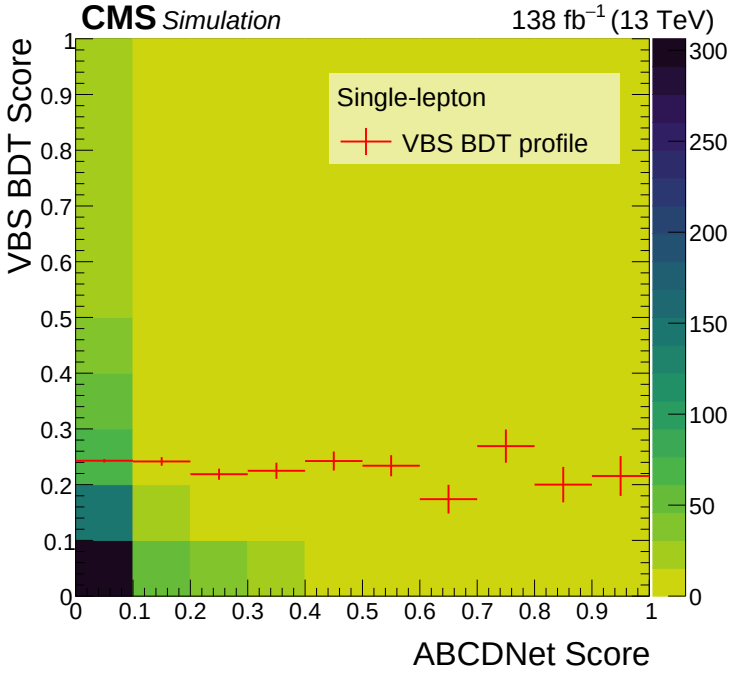

Figure B.4: Two-dimensional distribution of the DNN output and the VBS BDT output in the single-lepton channel, as obtained in background simulated events. These are the axes used in this channel to define the ABCD samples. A profile histogram is overlaid to better depict the statistical independence of the two variables.

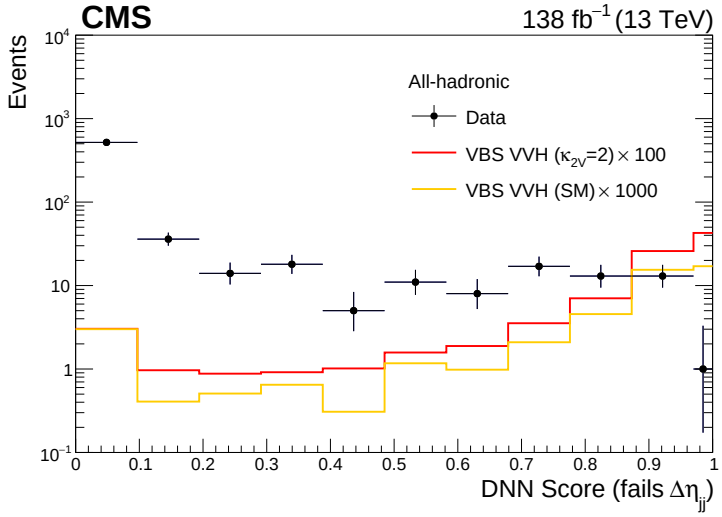

Figure B.5: Distribution of the DNN output in the regions B and D of the all-hadronic channel. The expected signals for the standard model scenario (orange) and for $\kappa_{2V} = 2$ (red) are superimposed to the data (black markers). The cross section used for signal is computed at leading order using MADGRAPH, and is scaled by a factor 1000 (100) for the SM ($\kappa_{2V} = 2$) signal to improve visibility.

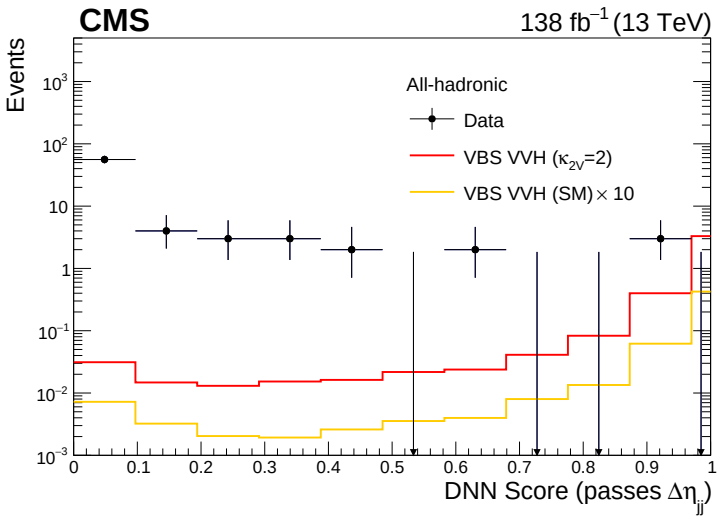

Figure B.6: Distribution of the DNN output in the regions A and C of the all-hadronic channel. The expected signals for the standard model scenario (orange) and for $\kappa_{2V} = 2$ (red) are superimposed to the data (black markers). The cross section used for signal is computed at leading order using MADGRAPH, and is scaled by a factor 10 for the SM signal to improve visibility.

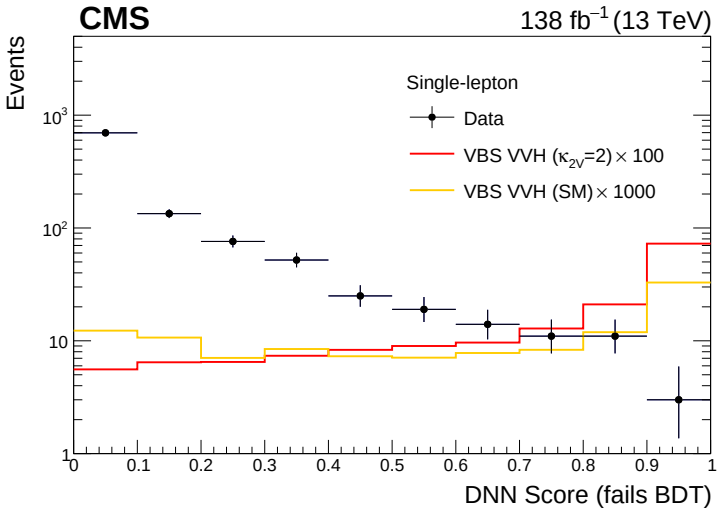

Figure B.7: Distribution of the DNN output in the regions B and D of the single-lepton channel. The expected signals for the standard model scenario (orange) and for $\kappa_{2V} = 2$ (red) are superimposed to the data (black markers). The cross section used for signal is computed at leading order using MADGRAPH, and is scaled by a factor 1000 (100) for the SM ($\kappa_{2V} = 2$) signal to improve visibility.

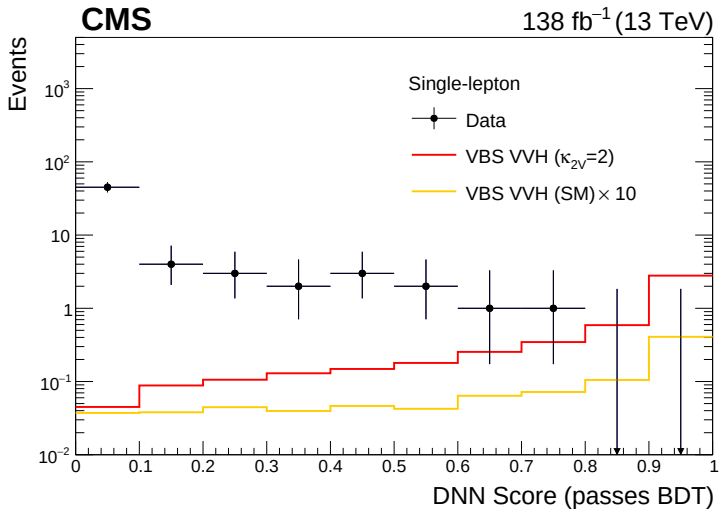

Figure B.8: Distribution of the DNN output in the regions A and C of the single-lepton channel. The expected signals for the standard model scenario (orange) and for $\kappa_{2V} = 2$ (red) are superimposed to the data (black markers). The cross section used for signal is computed at leading order using MADGRAPH, and is scaled by a factor 10 for the SM signal to improve visibility.

as a function of the κ_{2W} and κ_{2Z} coupling modifiers for each analysis channel. The expected and observed upper limits are shown in Fig. B.10 as a function of κ_{2W}. The upper limits as a function of κ_{2Z} are shown in Fig. B.11. The combined 95% CL upper limits are also shown.

Figure B.12 shows the two-dimensional expected and observed exclusion regions in the κ_{2W}-κ_{2Z} plane, corresponding to 2 standard deviations (σ), as obtained in each analysis channel. The exclusion regions obtained from the combination of all channels are also shown.

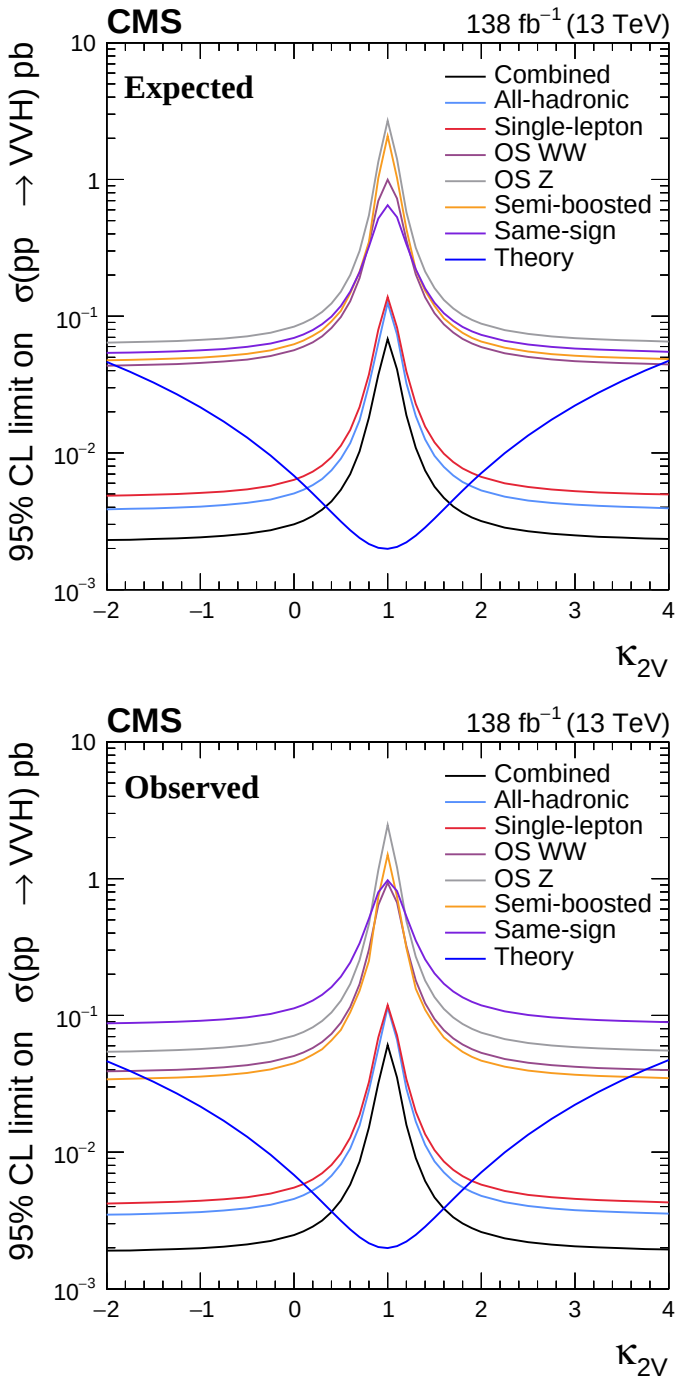

Figure B.9: Comparison of the expected (upper) and observed (lower) 95% CL limits on κ_{2V}. The combined limit is shown as in black, while the limits obtained in individual channels are shown as colored lines.

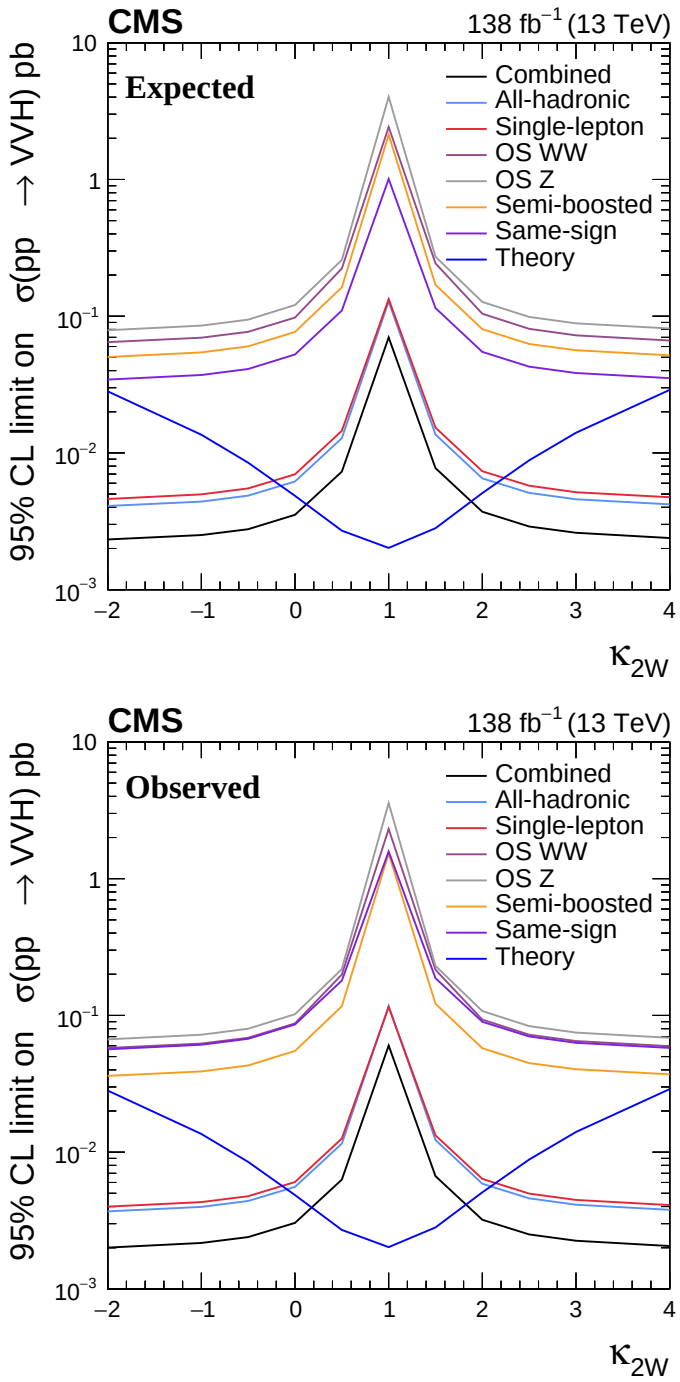

Figure B.10: Comparison of the expected (upper) and observed (lower) 95% CL limits on κ_{2W}. The combined limit is shown as in black, while the limits obtained in individual channels are shown as colored lines.

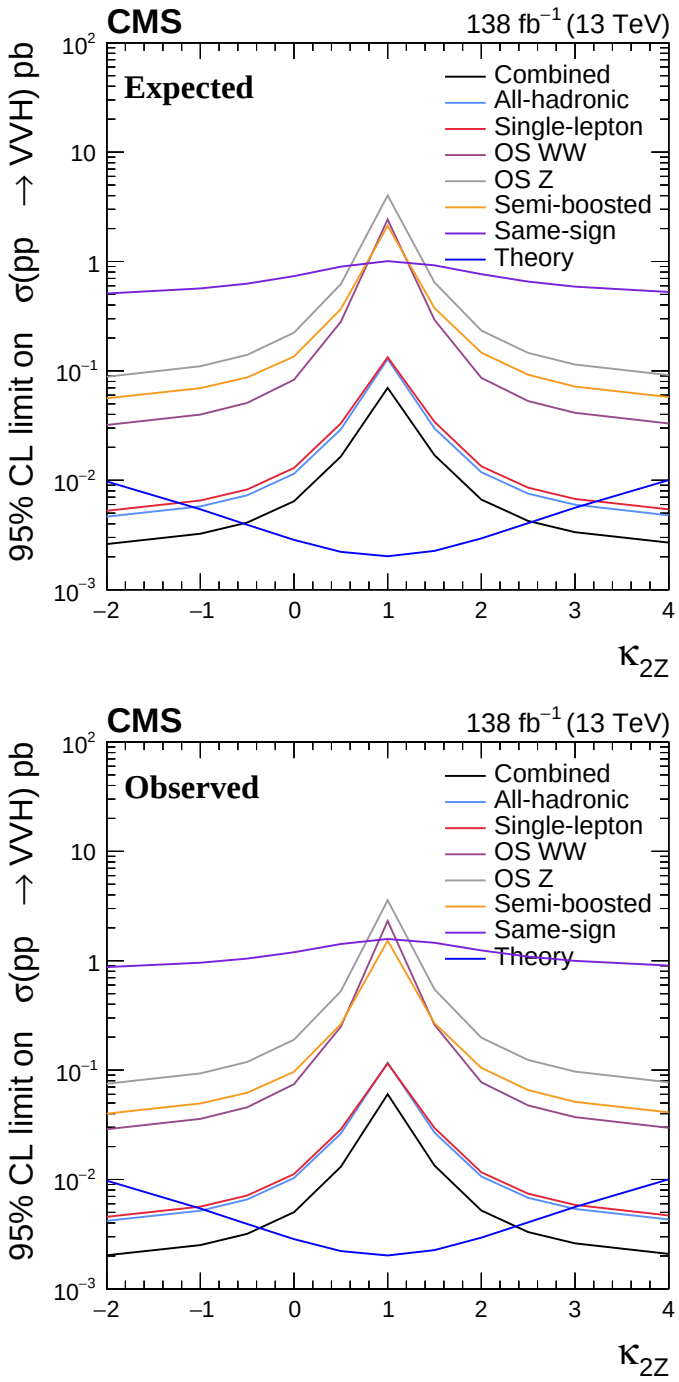

Figure B.11: Comparison of the expected (upper) and observed (lower) 95% CL limits on κ_{2Z}. The combined limit is shown as in black, while the limits obtained in individual channels are shown as colored lines.

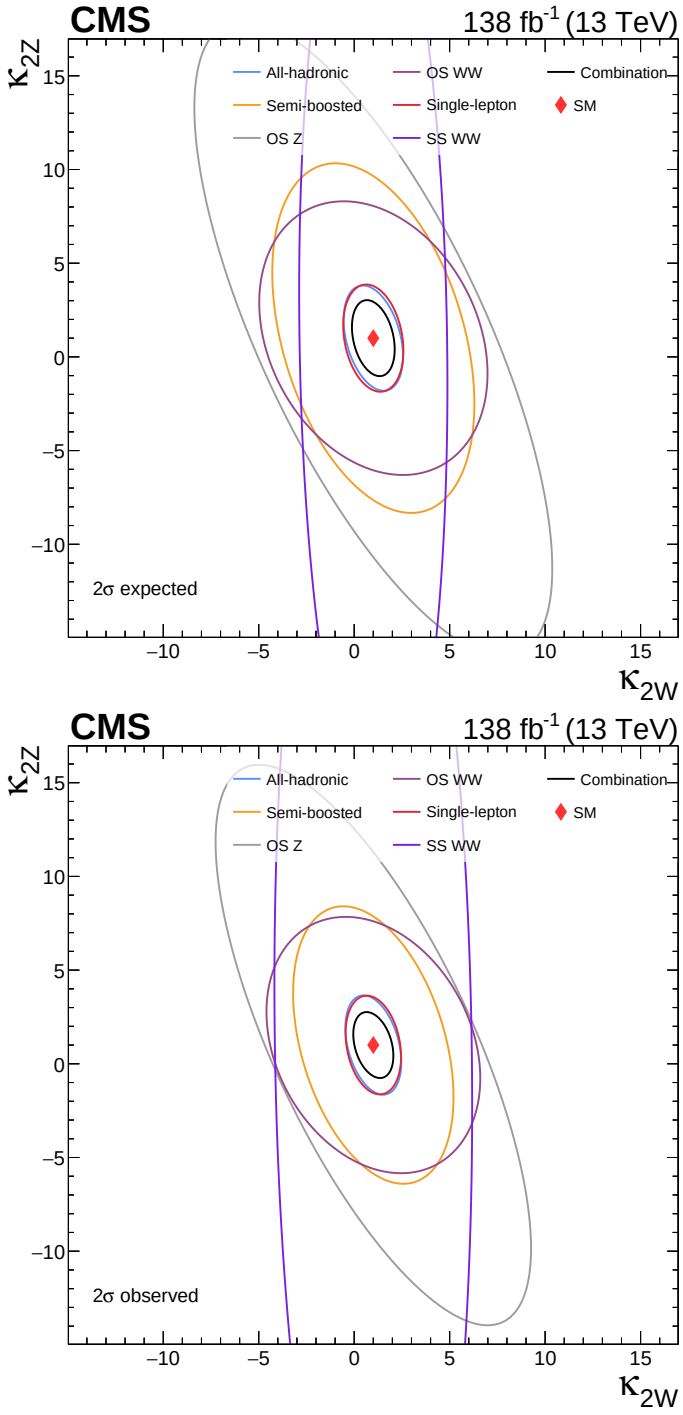

Figure B.12: Comparison of the expected (upper) and observed (lower) exclusion regions corresponding to 2 standard deviations (σ), in the two-dimensional κ_{2W}-κ_{2Z} plane. The combined exclusion region is shown as in black, while the exclusion regions obtained in individual channels are shown as colored lines.

C The CMS Collaboration

Yerevan Physics Institute, Yerevan, Armenia
A. Hayrapetyan, V. Makarenko, A. Tumasyan[1]

Institut für Hochenergiephysik, Vienna, Austria
W. Adam, L. Benato, T. Bergauer, M. Dragicevic, C. Giordano, P.S. Hussain, M. Jeitler[2], N. Krammer, A. Li, D. Liko, M. Matthewman, J. Schieck[2], R. Schöfbeck[2], M. Shooshtari, M. Sonawane, W. Waltenberger, C.E. Wulz[2]

Universiteit Antwerpen, Antwerpen, Belgium
T. Janssen, H. Kwon, D. Ocampo Henao, T. Van Laer, P. Van Mechelen

Vrije Universiteit Brussel, Brussel, Belgium
J. Bierkens, N. Breugelmans, J. D'Hondt, S. Dansana, A. De Moor, M. Delcourt, F. Heyen, Y. Hong, P. Kashko, S. Lowette, I. Makarenko, D. Müller, J. Song, S. Tavernier, M. Tytgat[3], G.P. Van Onsem, S. Van Putte, D. Vannerom

Université Libre de Bruxelles, Bruxelles, Belgium
B. Bilin, B. Clerbaux, A.K. Das, I. De Bruyn, G. De Lentdecker, H. Evard, L. Favart, P. Gianneios, A. Khalilzadeh, F.A. Khan, A. Malara, M.A. Shahzad, A. Sharma, L. Thomas, M. Vanden Bemden, C. Vander Velde, P. Vanlaer, F. Zhang

Ghent University, Ghent, Belgium
M. De Coen, D. Dobur, G. Gokbulut, D. Marckx, K. Skovpen, A.M. Tomaru, N. Van Den Bossche, J. van der Linden, J. Vandenbroeck, L. Wezenbeek

Université Catholique de Louvain, Louvain-la-Neuve, Belgium
H. Aarup Petersen, S. Bein, A. Benecke, A. Bethani, G. Bruno, A. Cappati, J. De Favereau De Jeneret, C. Delaere, F. Gameiro Casalinho, A. Giammanco, A.O. Guzel, V. Lemaitre, J. Lidrych, P. Malek, P. Mastrapasqua, S. Turkcapar

Centro Brasileiro de Pesquisas Fisicas, Rio de Janeiro, Brazil
G. Alves, M. Barroso Ferreira Filho, E. Coelho, C. Hensel, D. Matos Figueiredo, T. Menezes De Oliveira, C. Mora Herrera, P. Rebello Teles, M. Soeiro, E.J. Tonelli Manganote[4], A. Vilela Pereira

Universidade do Estado do Rio de Janeiro, Rio de Janeiro, Brazil
W.L. Aldá Júnior, H. Brandao Malbouisson, W. Carvalho, J. Chinellato[5], M. Costa Reis, E.M. Da Costa, G.G. Da Silveira[6], D. De Jesus Damiao, S. Fonseca De Souza, R. Gomes De Souza, S. Jesus, T. Laux Kuhn[6], M. Macedo, K. Mota Amarilo, L. Mundim, H. Nogima, J.P. Pinheiro, A. Santoro, A. Sznajder, M. Thiel, F. Torres Da Silva De Araujo[7]

Universidade Estadual Paulista (a), Universidade Federal do ABC (b), São Paulo, Brazil
C.A. Bernardes[6], L. Calligaris, F. Damas, E. De Moraes Gregores, B. Lopes Da Costa, I. Maietto Silverio, P.G. Mercadante, S.F. Novaes, B. Orzari, S. Padula, V. Scheurer, T. Tomei

Institute for Nuclear Research and Nuclear Energy, Bulgarian Academy of Sciences, Sofia, Bulgaria
A. Aleksandrov, G. Antchev, P. Danev, R. Hadjiiska, P. Iaydjiev, M. Shopova, G. Sultanov

University of Sofia, Sofia, Bulgaria
A. Dimitrov, L. Litov, B. Pavlov, P. Petkov, A. Petrov

Instituto de Alta Investigación, Universidad de Tarapacá, Arica, Chile
S. Keshri, D.N. Laroze Navarrete, S. Thakur

Universidad Técnica Federico Santa María, Valparaiso, Chile
W. Brooks

Beihang University, Beijing, China
T. Cheng, T. Javaid, L. Wang, L. Yuan

Department of Physics, Tsinghua University, Beijing, China
Z. Hu, Z. Liang, J. Liu, X. Wang, H. Yang

Institute of High Energy Physics, Beijing, China
G.M. Chen[8], H.S. Chen[8], M. Chen[8], Y. Chen, Q. Hou, X. Hou, F. Iemmi, C.H. Jiang, H. Liao, G. Liu, Z. Liu[9], J.n. Song[9], S. Song, J. Tao, C. Wang[8], J. Wang, H. Zhang, J. Zhao

State Key Laboratory of Nuclear Physics and Technology, Peking University, Beijing, China
A. Agapitos, Y. Ban, A. Carvalho Antunes De Oliveira, S. Deng, B. Guo, Q. Guo, C. Jiang, A. Levin, C. Li, Q. Li, Y. Mao, S. Qian, S.J. Qian, X. Qin, C. Quaranta, X. Sun, D. Wang, J. Wang, T. Yang, M. Zhang, Y. Zhao, C. Zhou

State Key Laboratory of Nuclear Physics and Technology, Institute of Quantum Matter, South China Normal University, Guangzhou, China, Guangzhou, China
S. Yang

Sun Yat-Sen University, Guangzhou, China
Z. You

University of Science and Technology of China, Hefei, China
K. Jaffel, N. Lu

Nanjing Normal University, Nanjing, China
G. Bauer[10,11], Z. Cui[11], B. Li[12], H. Wang, K. Yi[13], J. Zhang

Institute of Modern Physics and Key Laboratory of Nuclear Physics and Ion-beam Application (MOE) - Fudan University, Shanghai, China
Y. Li, Y. Zhou[14]

Zhejiang University - Department of Physics, Zhejiang, China
Z. Lin, C. Lu, M. Xiao[15]

Universidad de Los Andes, Bogota, Colombia
C. Avila, D.A. Barbosa Trujillo, A. Cabrera, C. Florez, J. Fraga, J.A. Reyes Vega

Universidad de Antioquia, Medellin, Colombia
C. Rendón, M. Rodriguez, A.A. Ruales Barbosa, J.D. Ruiz Alvarez

University of Split, Faculty of Electrical Engineering, Mechanical Engineering and Naval Architecture, Split, Croatia
N. Godinovic, D. Lelas, A. Sculac

University of Split, Faculty of Science, Split, Croatia
M. Kovac, A. Petkovic, T. Sculac

Institute Rudjer Boskovic, Zagreb, Croatia
P. Bargassa, V. Brigljevic, B.K. Chitroda, D. Ferencek, K. Jakovcic, A. Starodumov, T. Susa

University of Cyprus, Nicosia, Cyprus
A. Attikis, K. Christoforou, S. Konstantinou, C. Leonidou, L. Paizanos, F. Ptochos, P.A. Razis, H. Rykaczewski, H. Saka, A. Stepennov

Charles University, Prague, Czech Republic
M. Finger, M. Finger Jr.

Escuela Politecnica Nacional, Quito, Ecuador
E. Ayala

Universidad San Francisco de Quito, Quito, Ecuador
E. Carrera Jarrin

Academy of Scientific Research and Technology of the Arab Republic of Egypt, Egyptian Network of High Energy Physics, Cairo, Egypt
B. El-mahdy[16], E. Salama[17,18]

Center for High Energy Physics (CHEP-FU), Fayoum University, El-Fayoum, Egypt
A. Hussein, H. Mohammed

National Institute of Chemical Physics and Biophysics, Tallinn, Estonia
M. Kadastik, T. Lange, C. Nielsen, J. Pata, M. Raidal, N. Seeba, L. Tani

Department of Physics, University of Helsinki, Helsinki, Finland
E. Brücken, A. Milieva, K. Osterberg, M. Voutilainen

Helsinki Institute of Physics, Helsinki, Finland
F.I. Garcia Fuentes, P. Inkaew, K.T.S. Kallonen, R. Kumar Verma, T. Lampén, K. Lassila-Perini, B. Lehtela, S. Lehti, T. Lindén, N.R. Mancilla Xinto, M. Myllymäki, M.m. Rantanen, S. Saariokari, N.T. Toikka, J. Tuominiemi

Lappeenranta-Lahti University of Technology, Lappeenranta, Finland
N. Bin Norjoharuddeen, H. Kirschenmann, P.R. Luukka, H. Petrow

IRFU, CEA, Université Paris-Saclay, Gif-sur-Yvette, France
M. Besancon, F. Couderc, M. Dejardin, D. Denegri, P. Devouge, J.L. Faure, F. Ferri, P. Gaigne, S. Ganjour, P. Gras, G. Hamel de Monchenault, M. Kumar, V. Lohezic, Y. Maidannyk, J. Malcles, F. Orlandi, L. Portales, S. Ronchi, M.Ö. Sahin, A. Savoy-Navarro[19], P. Simkina, M. Titov, M. Tornago

Laboratoire Leprince-Ringuet, CNRS/IN2P3, Ecole Polytechnique, Institut Polytechnique de Paris, Palaiseau, France
R. Amella Ranz, F. Beaudette, G. Boldrini, P. Busson, C. Charlot, M. Chiusi, T.D. Cuisset, O. Davignon, A. De Wit, T. Debnath, I.T. Ehle, S. Ghosh, A. Gilbert, R. Granier de Cassagnac, L. Kalipoliti, M. Manoni, M. Nguyen, S. Obraztsov, C. Ochando, R. Salerno, J.B. Sauvan, Y. Sirois, G. Sokmen, L. Urda Gómez, A. Zabi, A. Zghiche

Institut Pluridisciplinaire Hubert Curien (IPHC), Université de Strasbourg, CNRS/IN2P3, Strasbourg, France
J.L. Agram[20], J. Andrea, D. Bloch, J.M. Brom, E.C. Chabert, C. Collard, G. Coulon, S. Falke, U. Goerlach, R. Haeberle, A.C. Le Bihan, M. Meena,

O. Poncet, G. Saha, P. Vaucelle

Centre de Calcul de l'Institut National de Physique Nucleaire et de Physique des Particules, CNRS/IN2P3, Villeurbanne, France
A. Di Florio

Institut de Physique des 2 Infinis de Lyon (IP2I), Villeurbanne, France
D. Amram, S. Beauceron, B. Blancon, G. Boudoul, N. Chanon, D. Contardo, P. Depasse, H. El Mamouni, J. Fay, S. Gascon, M. Gouzevitch, C. Greenberg, G. Grenier, B. Ille, E. Jourd'Huy, M. Lethuillier, B. Massoteau, L. Mirabito, A. Purohit, M. Vander Donckt, J. Xiao

Georgian Technical University, Tbilisi, Georgia
I. Bagaturia[21], I. Lomidze, Z. Tsamalaidze[22]

RWTH Aachen University, I. Physikalisches Institut, Aachen, Germany
V. Botta, S. Consuegra Rodríguez, L. Feld, K. Klein, M. Lipinski, P. Nattland, V. Oppenländer, A. Pauls, D. Pérez Adán, N. Röwert

RWTH Aachen University, III. Physikalisches Institut A, Aachen, Germany
C. Daumann, S. Diekmann, N. Eich, D. Eliseev, F. Engelke, J. Erdmann, M. Erdmann, B. Fischer, T. Hebbeker, K. Hoepfner, F. Ivone, A. Jung, N. Kumar, M.y. Lee, F. Mausolf, M. Merschmeyer, A. Meyer, A. Pozdnyakov, W. Redjeb, H. Reithler, U. Sarkar, V. Sarkisovi, A. Schmidt, C. Seth, A. Sharma, J.L. Spah, V. Vaulin, S. Zaleski

RWTH Aachen University, III. Physikalisches Institut B, Aachen, Germany
M.R. Beckers, C. Dziwok, G. Flügge, N. Hoeflich, T. Kress, A. Nowack, O. Pooth, A. Stahl, A. Zotz

Deutsches Elektronen-Synchrotron, Hamburg, Germany
A. Abel, M. Aldaya Martin, J. Alimena, S. Amoroso, Y. An, I. Andreev, J. Bach, S. Baxter, M. Bayatmakou, H. Becerril Gonzalez, O. Behnke, A. Belvedere, F. Blekman[23], K. Borras[24], A. Campbell, S. Chatterjee, L.X. Coll Saravia, G. Eckerlin, D. Eckstein, E. Gallo[23], A. Geiser, M. Guthoff, A. Hinzmann, L. Jeppe, M. Kasemann, C. Kleinwort, R. Kogler, M. Komm, D. Krücker, W. Lange, D. Leyva Pernia, K.y. Lin, K. Lipka[25], W. Lohmann[26], J. Malvaso, R. Mankel, I.A. Melzer-Pellmann, M. Mendizabal Morentin, A.B. Meyer, G. Milella, K. Moral Figueroa, A. Mussgiller, L.P. Nair, J. Niedziela, A. Nürnberg, J. Park, E. Ranken, A. Raspereza, D. Rastorguev, L. Rygaard, M. Scham[27,24], S. Schnake[24], C. Schwanenberger[23], D. Schwarz, P. Schütze, D. Selivanova, K. Sharko, M. Shchedrolosiev, D. Stafford, M. Torkian, A. Ventura Barroso, R. Walsh, D. Wang, Q. Wang, K. Wichmann, L. Wiens[24], C. Wissing, Y. Yang, S. Zakharov, A. Zimermmane Castro Santos

University of Hamburg, Hamburg, Germany
A.R. Alves Andrade, M. Antonello, S. Bollweg, M. Bonanomi, L. Ebeling, K. El Morabit, Y. Fischer, M. Frahm, E. Garutti, A. Grohsjean, A.A. Guvenli, J. Haller, D. Hundhausen, G. Kasieczka, P. Keicher, R. Klanner, W. Korcari, T. Kramer, C.c. Kuo, F. Labe, J. Lange, A. Lobanov, J. Matthiesen, L. Moureaux, K. Nikolopoulos, A. Paasch, K.J. Pena Rodriguez, N. Prouvost, B. Raciti, M. Rieger, D. Savoiu, P. Schleper, M. Schröder, J. Schwandt, M. Sommerhalder, H. Stadie, G. Steinbrück, R. Ward, B. Wiederspan, M. Wolf, C. Yede

Institut für Experimentelle Teilchenphysik, Karlsruhe, Germany
J. Ahäuser, S. Brommer, A. Brusamolino, E. Butz, Y.M. Chen, T. Chwalek, A. Dierlamm, G.G. Dincer, D. Druzhkin, U. Elicabuk, N. Faltermann, M. Giffels, A. Gottmann, F. Hartmann[28], M. Horzela, F. Hummer, U. Husemann, J. Kieseler, M. Klute, R. Kunnilan Muhammed Rafeek, O. Lavoryk, J.M. Lawhorn, A. Lintuluoto, S. Maier, A.A. Monsch, M. Mormile, T. Müller, E. Pfeffer, M. Presilla, G. Quast, K. Rabbertz, B. Regnery, R. Schmieder, N. Shadskiy, I. Shvetsov, H.J. Simonis, L. Sowa, L. Stockmeier, K. Tauqeer, M. Toms, B. Topko, N. Trevisani, C. Verstege, T. Voigtländer, R.F. Von Cube, J. Von Den Driesch, M. Wassmer, C. Winter, R. Wolf, W.D. Zeuner, X. Zuo

Institute of Nuclear and Particle Physics (INPP), NCSR Demokritos, Aghia Paraskevi, Greece
G. Anagnostou, G. Daskalakis, A. Kyriakis

National and Kapodistrian University of Athens, Athens, Greece
G. Melachroinos, Z. Painesis, I. Paraskevas, N. Saoulidou, K. Theofilatos, E. Tziaferi, E. Tzovara, K. Vellidis, I. Zisopoulos

National Technical University of Athens, Athens, Greece
T. Chatzistavrou, G. Karapostoli, K. Kousouris, E. Siamarkou, G. Tsipolitis

University of Ioánnina, Ioánnina, Greece
I. Bestintzanos, I. Evangelou, C. Foudas, P. Katsoulis, P. Kokkas, P.G. Kosmoglou Kioseoglou, N. Manthos, I. Papadopoulos, J. Strologas

HUN-REN Wigner Research Centre for Physics, Budapest, Hungary
C. Hajdu, D. Horvath[29,30], K. Márton, A.J. Rádl[31], F. Sikler, V. Veszpremi

MTA-ELTE Lendület CMS Particle and Nuclear Physics Group, Eötvös Loránd University, Budapest, Hungary
M. Csanad, K. Farkas, A. Fehérkuti[32], M.M.A. Gadallah[33], Á. Kadlecsik, M. León Coello, G. Pasztor, G.I. Veres

Faculty of Informatics, University of Debrecen, Debrecen, Hungary, Debrecen, Hungary
B. Ujvari, G. Zilizi

HUN-REN ATOMKI - Institute of Nuclear Research, Debrecen, Hungary
G. Bencze, S. Czellar, J. Molnar, Z. Szillasi

Karoly Robert Campus, MATE Institute of Technology, Gyongyos, Hungary
T.F. Csorgo[32], F. Nemes[32], T. Novak, I. Szanyi[34]

Indian Institute of Technology Bhubaneswar, Bhubaneswar, India
S. Bahinipati, S. Nayak, R. Raturi

Panjab University, Chandigarh, India
S. Bansal, S.B. Beri, V. Bhatnagar, S. Chauhan, N. Dhingra[35], A. Kaur, H. Kaur, M. Kaur, S. Kumar, T. Sheokand, J. Singh, A. Singla

University of Delhi, Delhi, India
A. Bhardwaj, A. Chhetri, B.C. Choudhary, A. Kumar, A. Kumar, M. Naimuddin, S. Phor, K. Ranjan, M.K. Saini

Indian Institute of Technology Mandi (IIT-Mandi), Himachal Pradesh, India
P. Palni

University of Hyderabad, Hyderabad, India
S. Acharya[36], B. Gomber

Indian Institute of Technology Kanpur, Kanpur, India
S. Mukherjee

Saha Institute of Nuclear Physics, HBNI, Kolkata, India
S. Bhattacharya, S. Das Gupta, S. Dutta, S. Dutta, S. Sarkar

Indian Institute of Technology Madras, Madras, India
M.M. Ameen, P.K. Behera, S. Chatterjee, G. Dash, A. Dattamunsi, P. Jana, P. Kalbhor, S. Kamble, J.R. Komaragiri[37], T. Mishra, P.R. Pujahari, A.K. Sikdar, R.K. Singh, P. Verma, S. Verma, A. Vijay

Indian lnstitute of Science Education and Research Mohali, Mohali, India
B.K. Sirasva

Tata Institute of Fundamental Research-A, Mumbai, India
L. Bhatt, S. Dugad, G.B. Mohanty, M. Shelake, P. Suryadevara

Tata Institute of Fundamental Research-B, Mumbai, India
A. Bala, S. Banerjee, S. Barman[38], R.M. Chatterjee, M. Guchait, S. Jain, A. Jaiswal, S. Kumar, M. Maity[38], G. Majumder, K. Mazumdar, S. Parolia, R. Saxena, A. Thachayath

National Institute of Science Education and Research, Jatni, Khorda, Odisha 752050, India Homi Bhabha National Institute, Training School Complex, Anushakti Nagar, Mumbai 400094, India, Odisha, India
D. Maity[39], P. Mal, K. Naskar[39], A. Nayak[39], K. Pal, P. Sadangi, S.K. Swain, S. Varghese[39], D. Vats[39]

Indian Institute of Science Education and Research (IISER), Pune, India
S. Dube, P. Hazarika, B. Kansal, A. Laha, R. Sharma, S. Sharma, K.Y. Vaish

Indian Institute of Technology Hyderabad, Telangana, India
S. Ghosh

Isfahan University of Technology, Isfahan, Iran
H. Bakhshiansohi[40], A. Jafari[41], V. Sedighzadeh Dalavi, M. Zeinali[42]

Institute for Research in Fundamental Sciences (IPM), Tehran, Iran
S. Bashiri, S. Chenarani[43], S.M. Etesami, Y. Hosseini, M. Khakzad, E. Khazaie, M. Mohammadi Najafabadi, S. Tizchang[44]

University College Dublin, Dublin, Ireland
M. Felcini, M. Grunewald

INFN Sezione di Bari[a], Università di Bari[b], Politecnico di Bari[c], Bari, Italy
M. Abbrescia[a,b], M. Barbieri[a,b], M. Buonsante[a,b], A. Colaleo[a,b], D. Creanza[a,c], N. De Filippis[a,c], M. De Palma[a,b], W. Elmetenawee[a,b,45], N. Ferrara[a,c], L. Fiore[a], L. Generoso[a,b], L. Longo[a], M. Louka[a,b], G. Maggi[a,c], M. Maggi[a], I. Margjeka[a], V. Mastrapasqua[a,b], S. My[a,b], F. Nenna[a,b], S. Nuzzo[a,b], A. Pellecchia[a,b], A. Pompili[a,b], G. Pugliese[a,c], R. Radogna[a,b], D. Ramos[a], A. Ranieri[a], L. Silvestris[a], F.M. Simone[a,c], A. Stamerra[a,b], Ü. Sözbilir[a], D. Troiano[a,b], R. Venditti[a,b], P. Verwilligen[a], A. Zaza[a,b]

INFN Sezione di Bologna[a], Università di Bologna[b], Bologna, Italy
G. Abbiendi[a], C. Battilana[a,b], P. Capiluppi[a,b], F.R. Cavallo[a], M. Cuffiani[a,b], G.M. Dallavalle[a], T. Diotalevi[a,b], F. Fabbri[a], A. Fanfani[a,b], R. Farinelli[a], D. Fasanella[a], P. Giacomelli[a], C. Grandi[a], L. Guiducci[a,b], S. Lo Meo[a,46], M. Lorusso[a,b], L. Lunerti[a], S. Marcellini[a], G. Masetti[a], F. Navarria[a,b], G. Paggi[a,b], A. Perrotta[a], A. Rossi[a,b], S. Rossi Tisbeni[a,b], T. Rovelli[a,b]

INFN Sezione di Catania[a], Università di Catania[b], Catania, Italy
S. Costa[a,b,47], A. Di Mattia[a], A. Lapertosa[a], R. Potenza[a,b], A. Tricomi[a,b,47]

INFN Sezione di Firenze[a], Università di Firenze[b], Firenze, Italy
J. Altork[a,b], P. Assiouras[a], G. Barbagli[a], G. Bardelli[a], M. Bartolini[a,b], A. Calandri[a,b], B. Camaiani[a,b], A. Cassese[a], R. Ceccarelli[a], V. Ciulli[a,b], C. Civinini[a], R. D'Alessandro[a,b], L. Damenti[a,b], E. Focardi[a,b], T. Kello[a], G. Latino[a,b], P. Lenzi[a,b], M. Lizzo[a], M. Meschini[a], S. Paoletti[a], A. Papanastassiou[a,b], G. Sguazzoni[a], L. Viliani[a]

INFN Laboratori Nazionali di Frascati, Frascati, Italy
L. Benussi, S. Colafranceschi[48], S. Meola[49], D. Piccolo

INFN Sezione di Genova[a], Università di Genova[b], Genova, Italy
M. Alves Gallo Pereira[a], F. Ferro[a], E. Robutti[a], S. Tosi[a,b]

INFN Sezione di Milano-Bicocca[a], Università di Milano-Bicocca, Milano[b], Milano-Bicocca, Italy
A. Benaglia[a], F. Brivio[a], V. Camagni[a,b], F. Cetorelli[a,b], F. De Guio[a,b], M.E. Dinardo[a,b], P. Dini[a], S. Gennai[a], R. Gerosa[a,b], A. Ghezzi[a,b], P. Govoni[a,b], L. Guzzi[a], M.R. Kim[a], G. Lavizzari[a,b], M.T. Lucchini[a,b], M. Malberti[a], S. Malvezzi[a], A. Massironi[a], D. Menasce[a], L. Moroni[a], M. Paganoni[a,b], S. Palluotto[a,b], D. Pedrini[a], A. Perego[a,b], G. Pizzati[a,b], T. Tabarelli de Fatis[a,b]

INFN Sezione di Napoli[a], Università di Napoli 'Federico II'[b], Università della Basilicata (Potenza)[c], Scuola Superiore Meridionale (SSM)[d], Napoli, Italy
S. Buontempo[a], C. Di Fraia[a,b], F. Fabozzi[a,c], L. Favilla[a,d], A.O.M. Iorio[a,b], L. Lista[a,b,50], P. Paolucci[a,28], B. Rossi[a]

INFN Sezione di Padova[a], Università di Padova[b], Universita degli Studi di Cagliari[c], Padova, Italy
P. Azzi[a], N. Bacchetta[a,51], M. Biasotto[a,52], D. Bisello[a,b], P. Bortignon[a,c], G. Bortolato[a,b], A.C.M. Bulla[a,c], R. Carlin[a,b], P. Checchia[a], T. Dorigo[a,53], U. Gasparini[a,b], S. Giorgetti[a], E. Lusiani[a], M. Margoni[a,b], A.T. Meneguzzo[a,b], J. Pazzini[a,b], F. Primavera[a,b], P. Ronchese[a,b], R. Rossin[a,b], F. Simonetto[a,b], M. Tosi[a,b], A. Triossi[a,b], M. Zanetti[a,b], P. Zotto[a,b], A. Zucchetta[a,b], G. Zumerle[a,b]

INFN Sezione di Pavia[a], Università di Pavia[b], Pavia, Italy
A. Braghieri[a], S. Calzaferri[a,b], P. Montagna[a,b], M. Pelliccioni[a,b], V. Re[a], C. Riccardi[a,b], P. Salvini[a], I. Vai[a,b], P. Vitulo[a,b]

INFN Sezione di Perugia[a], Università di Perugia[b], Perugia, Italy
S. Ajmal[a,b], M.E. Ascioti[a,b], G.M. Bilei[a], C. Carrivale[a,b], D. Ciangottini[a,b], L. Della Penna[a,b], L. Fanò[a,b], V. Mariani[a,b], M. Menichelli[a], F. Moscatelli[a,54], A. Rossi[a,b], A. Santocchia[a,b], D. Spiga[a], T. Tedeschi[a,b]

INFN Sezione di Pisa[a], Università di Pisa[b], Scuola Normale Superiore di Pisa[c], Università di Siena[d], Pisa, Italy
C. Aimè[a,b], C.A. Alexe[a,c], P. Asenov[a,b], P. Azzurri[a], G. Bagliesi[a], L. Bianchini[a,b], T. Boccali[a], E. Bossini[a], D. Bruschini[a,c], R. Castaldi[a], F. Cattafesta[a,c], M.A. Ciocci[a,d], M. Cipriani[a,b], R. Dell'Orso[a], S. Donato[a,b], R. Forti[a,b], A. Giassi[a], F. Ligabue[a,c], A.C. Marini[a,b], A. Messineo[a,b], S. Mishra[a], V.K. Muraleedharan Nair Bindhu[a,b], S. Nandan[a], F. Palla[a], M. Riggirello[a,c], A. Rizzi[a,b], G. Rolandi[a,c], S. Roy Chowdhury[a,55], T. Sarkar[a], A. Scribano[a], P. Solanki[a,b], P. Spagnolo[a], F. Tenchini[a,b], R. Tenchini[a], G. Tonelli[a,b], N. Turini[a,d], F. Vaselli[a,c], A. Venturi[a], P.G. Verdini[a]

INFN Sezione di Roma[a], Sapienza Università di Roma[b], Roma, Italy
P. Akrap[a,b], C. Basile[a,b], S.C. Behera[a], F. Cavallari[a], L. Cunqueiro Mendez[a,b], F. De Riggi[a,b], D. Del Re[a,b], E. Di Marco[a], M. Diemoz[a], F. Errico[a], L. Frosina[a,b], R. Gargiulo[a,b], B. Harikrishnan[a,b], F. Lombardi[a,b], E. Longo[a,b], L. Martikainen[a,b], J. Mijuskovic[a,b], G. Organtini[a,b], N. Palmeri[a,b], R. Paramatti[a,b], S. Rahatlou[a,b], C. Rovelli[a], F. Santanastasio[a,b], L. Soffi[a], V. Vladimirov[a,b]

INFN Sezione di Torino[a], Università di Torino[b], Università del Piemonte Orientale (Novara)[c], Torino, Italy
N. Amapane[a,b], R. Arcidiacono[a,c], S. Argiro[a,b], M. Arneodo[a,c], N. Bartosik[a,c], R. Bellan[a,b], A. Bellora[a,b], C. Biino[a], C. Borca[a,b], N. Cartiglia[a], M. Costa[a,b], R. Covarelli[a,b], N. Demaria[a], L. Finco[a], M. Grippo[a,b], B. Kiani[a,b], L. Lanteri[a,b], F. Legger[a], F. Luongo[a,b], C. Mariotti[a], S. Maselli[a], A. Mecca[a,b], L. Menzio[a,b], P. Meridiani[a], E. Migliore[a,b], M. Monteno[a], M.M. Obertino[a,b], G. Ortona[a], L. Pacher[a,b], N. Pastrone[a], M. Ruspa[a,c], F. Siviero[a,b], V. Sola[a,b], A. Solano[a,b], A. Staiano[a], C. Tarricone[a,b], D. Trocino[a], G. Umoret[a,b], E. Vlasov[b], R. White[a,b]

INFN Sezione di Trieste[a], Università di Trieste[b], Trieste, Italy
J. Babbar[a,b,55], S. Belforte[a], V. Candelise[a,b], M. Casarsa[a], F. Cossutti[a], K. De Leo[a], G. Della Ricca[a,b], R. Delli Gatti[a,b]

Kyungpook National University, Daegu, Korea
S. Dogra, J. Hong, J. Kim, T. Kim, D. Lee, H. Lee, J. Lee, S.W. Lee, C.S. Moon, Y.D. Oh, S. Sekmen, B. Tae, Y.C. Yang

Department of Mathematics and Physics - Gangneung-Wonju National University, Gangneung, Korea
M.S. Kim

Chonnam National University, Institute for Universe and Elementary Particles, Kwangju, Korea
G. Bak, P. Gwak, H. Kim, D.H. Moon, J. Seo

Hanyang University, Seoul, Korea
E. Asilar, F. Carnevali, J. Choi[56], T.J. Kim, Y. Ryou

Korea University, Seoul, Korea
S. Ha, S. Han, B.S. Hong, J. Kim, K. Lee, K.S. Lee, S. Lee, J. Yoo

Kyung Hee University, Department of Physics, Seoul, Korea
J. Goh, J. Shin, S. Yang

Sejong University, Seoul, Korea

Y. Kang, H. Kim, Y. Kim, B. Ko, S. Lee

Seoul National University, Seoul, Korea
J. Almond, J.H. Bhyun, J. Choi, J. Choi, W. Jun, H. Kim, J. Kim, T. Kim, Y. Kim, Y.W. Kim, S. Ko, H. Lee, J. Lee, J. Lee, B.H. Oh, J. Shin, U. Yang, I. Yoon

University of Seoul, Seoul, Korea
W. Jang, D.Y. Kang, D. Kim, S. Kim, J.S.H. Lee, Y. Lee, I. Park, Y. Roh, I. J. Watson

Yonsei University, Department of Physics, Seoul, Korea
G. Cho, K. Hwang, B. Kim, S. Kim, K. Lee, H.D. Yoo

Sungkyunkwan University, Suwon, Korea
Y. Lee, I. Yu

College of Engineering and Technology, American University of the Middle East (AUM), Dasman, Kuwait
T. Beyrouthy, Y. Gharbia

Kuwait University - College of Science - Department of Physics, Safat, Kuwait
F. Alazemi

Riga Technical University, Riga, Latvia
K. Dreimanis, O.M. Eberlins, A. Gaile, C. Munoz Diaz, D. Osite, G. Pikurs, R. Plese, A. Potrebko, M. Seidel, D. Sidiropoulos Kontos

University of Latvia (LU), Riga, Latvia
N.R. Strautnieks

Vilnius University, Vilnius, Lithuania
M. Ambrozas, A. Juodagalvis, S. Nargelas, A. Rinkevicius, G. Tamulaitis

National Centre for Particle Physics, Universiti Malaya, Kuala Lumpur, Malaysia
I. Yusuff[57], Z. Zolkapli

University of Sonora (UNISON), Hermosillo, Mexico
J.F. Benitez, A. Castaneda Hernandez, A. Cota Rodriguez, L.E. Cuevas Picos, H.A. Encinas Acosta, L.G. Gallegos Maríñez, J.A. Murillo Quijada, L. Valencia Palomo

Centro de Investigacion y de Estudios Avanzados del IPN, Mexico City, Mexico
G. Ayala, H. Castilla-Valdez, H. Crotte Ledesma, R. Lopez-Fernandez, J. Mejia Guisao, R. Reyes-Almanza, A. Sánchez Hernández

Universidad Iberoamericana, Mexico City, Mexico
C. Oropeza Barrera, D.L. Ramirez Guadarrama, M. Ramírez García

Benemerita Universidad Autonoma de Puebla, Puebla, Mexico
I. Bautista, F.E. Neri Huerta, I. Pedraza, H.A. Salazar Ibarguen, C. Uribe Estrada

University of Montenegro, Podgorica, Montenegro
I. Bubanja, N. Raicevic

University of Canterbury, Christchurch, New Zealand
P.H. Butler

National Centre for Physics, Quaid-I-Azam University, Islamabad, Pakistan
A. Ahmad, M.I. Asghar, A. Awais, M.I.M. Awan, W.A. Khan

AGH University of Krakow, Krakow, Poland
V. Avati, L. Forthomme, L. Grzanka, M. Malawski, K. Piotrzkowski

National Centre for Nuclear Research, Swierk, Poland
M. Bluj, M. Górski, M. Kazana, M. Szleper, P. Zalewski

Institute of Experimental Physics, Faculty of Physics, University of Warsaw, Warsaw, Poland
K. Bunkowski, K. Doroba, A. Kalinowski, M. Konecki, J. Krolikowski, A. Muhammad

Warsaw University of Technology, Warsaw, Poland
P. Fokow, K. Pozniak, W. Zabolotny

Laboratório de Instrumentação e Física Experimental de Partículas, Lisboa, Portugal
M. Araujo, D. Bastos, C. Beirão Da Cruz E Silva, A. Boletti, M. Bozzo, T. Camporesi, G. Da Molin, M. Gallinaro, J. Hollar, N. Leonardo, G.B. Marozzo, A. Petrilli, M. Pisano, J. Seixas, J. Varela, J.W. Wulff

Joint Institute for Nuclear Research, Dubna, Russia
S. Afanasiev, V. Alexakhin, Y. Andreev, T. Aushev, D. Budkouski, R. Chistov, M. Danilov, T. Dimova, A. Ershov, S. Gninenko, I. Gorbunov, A. Gribushin, A. Kamenev, V. Karjavine, M. Kirsanov, V. Klyukhin, O. Kodolova[58], V. Korenkov, I. Korsakov, A. Kozyrev, N. Krasnikov, A. Lanev, A. Malakhov, V. Matveev, A. Nikitenko[59,58], V. Palichik, V. Perelygin, S. Petrushanko, O. Radchenko, M. Savina, V. Shalaev, S. Shmatov, S. Shulha, Y. Skovpen, K. Slizhevskiy, V. Smirnov, O. Teryaev, I. Tlisova, A. Toropin, N. Voytishin, A. Zarubin, I. Zhizhin

Skobeltsyn Institute of Nuclear Physics, Lomonosov Moscow State University, Moscow, Russia
E. Boos, V. Bunichev, M. Dubinin[60], V. Savrin, A. Snigirev

Faculty of Physics, University of Belgrade, Belgrade, Serbia
P. Adzic, L. Markovic, P. Milenovic, V. Milosevic

Vinca Institute of Nuclear Science, Belgrade, Serbia
D. Devetak, M. Dordevic, J. Milosevic, L. Nadderd, V. Rekovic, M. Stojanovic

Centro de Investigaciones Energéticas Medioambientales y Tecnológicas (CIEMAT), Madrid, Spain
M. Alcalde Martinez, J. Alcaraz Maestre, J.A. Brochero Cifuentes, M. Cepeda, M. Cerrada, N. Colino, B. De La Cruz, A. Delgado Peris, A. Escalante Del Valle, C. Fernandez Bedoya, D. Fernández Del Val, J.P. Fernández Ramos, J. Flix, M.C. Fouz, M. Gonzalez Hernandez, O. Gonzalez Lopez, S. Goy Lopez, J.M. Hernandez, M.I. Josa, J. Llorente Merino, O. Manzanilla, C. Martin Perez, E. Martin Viscasillas, D. Moran, C.M. Morcillo Perez, Á. Navarro Tobar, R. Paz Herrera, J. Puerta Pelayo, A.M. Pérez-Calero Yzquierdo, I. Redondo, J. Vazquez Escobar

Universidad Autónoma de Madrid, Madrid, Spain
J.F. de Trocóniz

Universidad de Oviedo, Instituto Universitario de Ciencias y Tecnologías Espaciales de Asturias (ICTEA), Oviedo, Spain
B. Alvarez Gonzalez, J. Ayllon Torresano, A. Cardini, J. Cuevas, J. Del Riego Badas,

D. Estrada Acevedo, J. Fernandez Menendez, S. Folgueras, I. Gonzalez Caballero, P. Leguina, M. Obeso Menendez, E. Palencia Cortezon, J. Prado Pico, A. Soto Rodríguez, P. Vischia

Instituto de Física de Cantabria (IFCA), CSIC-Universidad de Cantabria, Santander, Spain
S. Blanco Fernández, I.J. Cabrillo, A. Calderon, J. Duarte Campderros, M. Fernandez, G. Gomez, C. Lasaosa García, R. Lopez Ruiz, C. Martinez Rivero, P. Martinez Ruiz del Arbol, F. Matorras, P. Matorras Cuevas, E. Navarrete Ramos, J. Piedra Gomez, C. Quintana San Emeterio, L. Scodellaro, I. Vila, R. Vilar Cortabitarte, J.M. Vizan Garcia

University of Colombo, Colombo, Sri Lanka
D.C.W. Dhammage, B. Kailasapathy[61]

University of Ruhuna, Department of Physics, Matara, Sri Lanka
W.G. Dharmaratna[62], K. Liyanage, N. Perera

CERN, European Organization for Nuclear Research, Geneva, Switzerland
D. Abbaneo, C. Amendola, R. Ardino, E. Auffray, J. Baechler, D. Barney, J. Bendavid, M. Bianco, A. Bocci, L. Borgonovi, C. Botta, A. Bragagnolo, C.E. Brown, C. Caillol, G. Cerminara, P. Connor, K. Cormier, D. D'Enterria, A. Dabrowski, A. David Tinoco Mendes, A. De Roeck, M.M. Defranchis, M. Deile, M. Dobson, P.J. Fernández Manteca, B.A. Fontana Santos Alves, E. Fontanesi, W. Funk, A. Gaddi, S. Giani, D. Gigi, K. Gill, F. Glege, M. Glowacki, A. Gruber, J. Hegeman, J.K. Heikkilä, R. Hofsaess, B. Huber, T. James, P. Janot, O. Kaluzinska, O. Karacheban[26], G. Karathanasis, S. Laurila, P. Lecoq, E. Leutgeb, C. Lourenco, A.m. Lyon, M. Magherini, L. Malgeri, M. Mannelli, A. Mehta, F. Meijers, J.A. Merlin, S. Mersi, E. Meschi, M. Migliorini, F. Monti, F. Moortgat, M. Mulders, M. Musich, I. Neutelings, S. Orfanelli, F. Pantaleo, M. Pari, G. Petrucciani, A. Pfeiffer, M. Pierini, M. Pitt, H. Qu, D. Rabady, A. Reimers, B. Ribeiro Lopes, F. Riti, P. Rosado, M. Rovere, H. Sakulin, R. Salvatico, S. Sanchez Cruz, S. Scarfi, M. Selvaggi, K. Shchelina, P. Silva, P. Sphicas[63], A.G. Stahl Leiton, A. Steen, S. Summers, D. Treille, P. Tropea, E. Vernazza, J. Wanczyk[64], S. Wuchterl, M. Zarucki, P. Zehetner, P. Zejdl, G. Zevi Della Porta

Synthetic Institute for people with CERN contract, Geneva, Switzerland
L. Dudko, V. Kim[65], V. Murzin, V. Oreshkin, D. Sosnov

PSI Center for Neutron and Muon Sciences, Villigen, Switzerland
T. Bevilacqua[66], L. Caminada[66], W. Erdmann, R. Horisberger, Q. Ingram, H.C. Kaestli, D. Kotlinski, C. Lange, U. Langenegger, A. Nigamova, L. Noehte[66], T. Rohe, A. Samalan

ETH Zurich - Institute for Particle Physics and Astrophysics (IPA), Zurich, Switzerland
T.K. Aarrestad, M. Backhaus, G. Bonomelli, C. Cazzaniga, K. Datta, P. De Bryas Dexmiers D'Archiacchiac[64], A. De Cosa, G. Dissertori, M. Dittmar, M. Donegà, F. Glessgen, C. Grab, T.G. Harte, N. Härringer, W. Lustermann, M. Malucchi, R.A. Manzoni, L. Marchese, A. Mascellani[64], F. Nessi-Tedaldi, F. Pauss, B. Ristic, R. Seidita, J. Steggemann[64], A. Tarabini, D. Valsecchi, R. Wallny

Universität Zürich, Zurich, Switzerland

C. Amsler[67], F. Bilandzija, P. Bärtschi, M.F. Canelli, G. Celotto, V. Guglielmi, A. Jofrehei, B. Kilminster, T.H. Kwok, S. Leontsinis, V. Lukashenko, A. Macchiolo, F. Meng, M. Missiroli, J. Motta, P. Robmann, E. Shokr, F. Stäger, R. Tramontano, P. Viscone

Çukurova University, Adana, Türkiye
D. Agyel, F. Dolek, I. Dumanoglu[68], Y. Guler[69], E. Gurpinar Guler[69], C. Isik, O. Kara[70], A. Kayis Topaksu, Y. Komurcu, G. Onengut, K. Ozdemir[71], B. Tali[72], U.G. Tok, E. Uslan, I.S. Zorbakir

Hacettepe University, Ankara, Türkiye
S. Sen

Middle East Technical University, Physics Department, Ankara, Türkiye
M. Yalvac[73]

Bogazici University, Istanbul, Türkiye
B. Akgun, I.O. Atakisi[74], E. Gülmez, M. Kaya[75], O. Kaya[76], M.A. Sarkisla[77], S. Tekten[78]

Istanbul Technical University, Istanbul, Türkiye
D. Boncukcu, A. Cakir, K. Cankocak[68,79]

Istanbul University, Istanbul, Türkiye
B. Hacisahinoglu, I. Hos[80], B. Kaynak, S. Ozkorucuklu, O. Potok, H. Sert, C. Simsek, C. Zorbilmez

Yildiz Technical University, Istanbul, Türkiye
S. Cerci, C. Dozen[81], B. Isildak, E. Simsek, D. Sunar Cerci, T. Yetkin[81]

National Central University, Chung-Li, Taiwan
D. Bhowmik, C.M. Kuo, P.K. Rout, S. Taj, P.C. Tiwari[37]

National Taiwan University (NTU), Taipei, Taiwan
L. Ceard, K.F. Chen, Z.g. Chen, A. De Iorio, G.W.S. Hou, T.h. Hsu, Y.w. Kao, S. Karmakar, G. Kole, Y.y. Li, R.S. Lu, E. Paganis, X.f. Su, J. Thomas-Wilsker, L.s. Tsai, D. Tsionou, H.y. Wu, E. Yazgan

High Energy Physics Research Unit, Department of Physics, Faculty of Science, Chulalongkorn University, Bangkok, Thailand
C. Asawatangtrakuldee, N. Srimanobhas

Tunis El Manar University, Tunis, Tunisia
Y. Maghrbi

Institute for Scintillation Materials of National Academy of Science of Ukraine, Kharkiv, Ukraine
A. Boyaryntsev, O. Dadazhanova, B. Grynyov

National Science Centre, Kharkiv Institute of Physics and Technology, Kharkiv, Ukraine
L. Levchuk

University of Bristol, Bristol, United Kingdom
J.J. Brooke, A. Bundock, F.J.J. Bury, E. Clement, D. Cussans, D. Dharmender, H. Flacher, J. Goldstein, H.F. Heath, M.l. Holmberg, L. Kreczko, S. Paramesvaran, L. Robertshaw, M.S. Sanjrani[40], J. Segal, V.J. Smith

Rutherford Appleton Laboratory, Didcot, United Kingdom
A. Ball, K.W. Bell, A. Belyaev[82], C. Brew, R.M. Brown, D.J. Cockerill, A. Elliot, K.V. Ellis, J. Gajownik, K. Harder, S. Harper, J. Linacre, K. Manolopoulos, M. Moallemi, D.M. Newbold, E. Olaiya, D. Petyt, T. Reis, A.R. Sahasransu, G. Salvi, T. Schuh, C. Shepherd-Themistocleous, I.R. Tomalin, K.C. Whalen, T. Williams

Imperial College, London, United Kingdom
I. Andreou, R. Bainbridge, P. Bloch, O. Buchmuller, C.A. Carrillo Montoya, D. Colling, I. Das, P. Dauncey, G. Davies, M. Della Negra, S. Fayer, G. Fedi, G. Hall, H.R. Hoorani, A. Howard, G. Iles, C.R. Knight, P. Krueper, J. Langford, K.H. Law, J. León Holgado, L. Lyons, A.M. Magnan, B. Maier, S. Mallios, A. Mastronikolis, M. Mieskolainen, J. Nash[83], M. Pesaresi, P.B. Pradeep, B.C. Radburn-Smith, A. Richards, A. Rose, L. Russell, K. Savva, C. Seez, R. Shukla, A. Tapper, K. Uchida, G.P. Uttley, T. Virdee[28], M. Vojinovic, N. Wardle, D. Winterbottom

Brunel University, Uxbridge, United Kingdom
J. Cole, A. Khan, P. Kyberd, I. Reid

The University of Alabama, Tuscaloosa, Alabama, USA
B. Bam, A. Buchot Perraguin, S. Campbell, R. Chudasama, S. Cooper, C. Crovella, G. Fidalgo, S.V. Gleyzer, A. Khukhunaishvili, K. Matchev, E. Pearson, P. Rumerio[84], E. Usai, R. Yi

University of California, Davis, Davis, California, USA
S. Abbott, S. Baradia, B. Barton, R. Breedon, H. Cai, M. Calderon De La Barca Sanchez, E. Cannaert, M. Chertok, M. Citron, J. Conway, P.T. Cox, F. Eble, R. Erbacher, O. Kukral, G. Mocellin, S. Ostrom, I. Salazar Segovia, J.S. Tafoya Vargas, W. Wei, S. Yoo

University of California, San Diego, La Jolla, California, USA
A. Aportela, A. Arora, J.G. Branson, S. Cittolin, S. Cooperstein, B. D'Anzi, D. Diaz, J. Duarte, L. Giannini, Y. Gu, J. Guiang, V. Krutelyov, R. Lee, J. Letts, H. Li, M. Masciovecchio, F. Mokhtar, S. Mukherjee, M. Pieri, D. Primosch, M. Quinnan, V. Sharma, M. Tadel, E. Vourliotis, F. Würthwein, A. Yagil, Z. Zhao

University of California, Los Angeles, California, USA
K. Adamidis, M. Bachtis, D. Campos, R. Cousins, S. Crossley, G. Flores Avila, J. Hauser, M. Ignatenko, M.A. Iqbal, T. Lam, Y.f. Lo, E. Manca, A. Nunez Del Prado, D. Saltzberg, V. Valuev

California Institute of Technology, Pasadena, California, USA
A. Albert, S. Bhattacharya, A. Bornheim, O. Cerri, R. Kansal, J. Mao, H.B. Newman, G. Reales Gutiérrez, T. Sievert, M. Spiropulu, J.R. Vlimant, R.A. Wynne, S. Xie

University of California, Riverside, Riverside, California, USA
R. Clare, J.W. Gary, G. Hanson

University of California, Santa Barbara - Department of Physics, Santa Barbara, California, USA
A. Barzdukas, L. Brennan, C. Campagnari, S. Carron Montero[85], K. Downham, C. Grieco, M.M. Hussain, J. Incandela, M.W.K. Lai, A.J. Li, P. Masterson,

J. Richman, S.N. Santpur, R. Schmitz, D. Stuart, T.Á. Vámi, X. Yan, D. Zhang

University of Colorado Boulder, Boulder, Colorado, USA
J.P. Cumalat, W.T. Ford, A. Hart, S. Kwan, J. Pearkes, C. Savard, N. Schonbeck, K. Stenson, K. Ulmer, S.R. Wagner, N. Zipper, D. Zuolo

The Catholic University of America, Washington, DC, USA
R. Bartek, A. Dominguez, S. Raj, B. Sahu[36], A.E. Simsek, S.S. Yu

University of Florida, Gainesville, Florida, USA
C. Aruta, P. Avery, D. Bourilkov, P. Chang, V. Cherepanov, R.D. Field, C. Huh, E. Koenig, M. Kolosova, J. Konigsberg, A. Korytov, G. Mitselmakher, K. Mohrman, A. Muthirakalayil Madhu, N. Rawal, S. Rosenzweig, V. Sulimov, Y. Takahashi, J. Wang, E.M.A. Zenhom

Florida Institute of Technology, Melbourne, Florida, USA
B. Alsufyani, S. Butalla, S. Das, M. Hohlmann, M. Lavinsky, E. Yanes

Florida State University, Tallahassee, Florida, USA
T. Adams, A. Al Kadhim, A. Askew, S. Bower, R. Goff, R. Hashmi, A. Hassani, R.S. Kim, T. Kolberg, G. Martinez, M. Mazza, H. Prosper, P.R. Prova, R. Yohay

Fermi National Accelerator Laboratory, Batavia, Illinois, USA
M. Albrow, M. Alyari, O. Amram, G. Apollinari, A. Apresyan, L.A. Bauerdick, D. Berry, J. Berryhill, P.C. Bhat, K. Burkett, J.N. Butler, A. Canepa, G.B. Cerati, H. Cheung, F. Chlebana, C. Cosby, G. Cummings, I. Dutta, V.D. Elvira, J. Freeman, A. Gandrakota, Z. Gecse, L. Gray, D. Green, A. Grummer, S. Grünendahl, D. Guerrero, O. Gutsche, R.M. Harris, J. Hirschauer, V. Innocente, B. Jayatilaka, S. Jindariani, M. Johnson, U. Joshi, B. Klima, S. Lammel, C. Lee, D. Lincoln, R. Lipton, T. Liu, K. Maeshima, D. Mason, P. McBride, P. Merkel, S. Mrenna, S. Nahn, J. Ngadiuba, D. Noonan, S. Norberg, V. Papadimitriou, N. Pastika, K. Pedro, C. Pena[60], C.E. Perez Lara, V. Perovic, F. Ravera, A. Reinsvold Hall[86], L. Ristori, M. Safdari, E. Sexton-Kennedy, E. Smith, N. Smith, A. Soha, L. Spiegel, S. Stoynev, J. Strait, L. Taylor, S. Tkaczyk, N.V. Tran, L. Uplegger, E.W. Vaandering, C. Wang, I. Zoi

University of Illinois Chicago, Chicago, Illinois, USA
M.R. Adams, N. Barnett, A. Baty, C. Bennett, R. Cavanaugh, R. Escobar Franco, O. Evdokimov, C.E. Gerber, H. Gupta, M. Hawksworth, A. Hingrajiya, D.J. Hofman, Z. Huang, J.h. Lee, C. Mills, S. Nanda, G. Nigmatkulov, B. Ozek, T. Phan, D. Pilipovic, R. Pradhan, E. Prifti, P. Roy, T. Roy, D. Shekar, N. Singh, A. Thielen, M. Tonjes, N. Varelas, M.A. Wadud, J. Yoo

Northwestern University, Evanston, Illinois, USA
S. Dittmer, K.A. Hahn, M. Mcginnis, Y. Miao, D.G. Monk, M.H. Schmitt, A. Taliercio, M. Velasco, J. Wang

Purdue University Northwest, Hammond, Indiana, USA
N. Parashar, A. Pathak, E. Shumka

University of Notre Dame, Notre Dame, Indiana, USA
G. Agarwal, R. Band, R. Bucci, S. Castells, A. Das, A. Datta, A. Ehnis, R. Goldouzian, M. Hildreth, K. Hurtado Anampa, T. Ivanov, C. Jessop, A. Karneyeu, K. Lannon, J. Lawrence, N. Loukas, D. Lutton, J. Mariano,

N. Marinelli, T. McCauley, C. Mcgrady, C. Moore, Y. Musienko[87], H. Nelson, M. Osherson, A. Piccinelli, R. Ruchti, A. Townsend, Y. Wan, M. Wayne, H. Yockey

Purdue University, West Lafayette, Indiana, USA
S. Chandra, A. Gu, L. Gutay, M. Huwiler, M. Jones, A.W. Jung, D. Kondratyev, J. Li, M. Liu, G. Negro, N. Neumeister, G. Paspalaki, S. Piperov, N.R. Saha, J.F. Schulte, F. Wang, A. Wildridge, W. Xie, Y. Yao, Y. Zhong

The University of Iowa, Iowa City, Iowa, USA
M. Alhusseini, D. Blend, K. Dilsiz[88], O.K. Köseyan, A. Mestvirishvili[89], O. Neogi, H. Ogul[90], Y. Onel, A. Penzo, C. Snyder, E. Tiras[91]

The University of Kansas, Lawrence, Kansas, USA
A. Abreu, L.F. Alcerro Alcerro, J. Anguiano, S. Arteaga Escatel, P. Baringer, A. Bean, R. Bhattacharya, Z. Flowers, D. Grove, J. King, G. Krintiras, M. Lazarovits, C. Le Mahieu, J. Marquez, M. Murray, M. Nickel, S. Popescu[92], C. Rogan, C. Royon, S. Rudrabhatla, S. Sanders, C. Smith, G. Wilson

Kansas State University, Manhattan, Kansas, USA
B. Allmond, N. Islam, A. Ivanov, K. Kaadze, Y. Maravin, J. Natoli, G.G. Reddy, D. Roy, G. Sorrentino

Johns Hopkins University, Baltimore, Maryland, USA
B. Blumenfeld, J. Davis, A. Gritsan, L. Kang, S. Kyriacou, P. Maksimovic, M. Roguljic, S. Sekhar, M.V. Srivastav, M. Swartz

University of Maryland, College Park, Maryland, USA
D. Baden, A. Belloni, J. Bistany-riebman, S.C. Eno, N.J. Hadley, S. Jabeen, R.G. Kellogg, T. Koeth, B. Kronheim, S. Lascio, P. Major, A. Mignerey, C. Palmer, C. Papageorgakis, M.M. Paranjpe, E. Popova[93], A. Shevelev, L. Zhang

Boston University, Boston, Massachusetts, USA
S. Cholak, G. De Castro, Z. Demiragli, C. Erice, C. Fangmeier, C. Fernandez Madrazo, J. Fulcher, F. Golf, S. Jeon, J. O'Cain, I. Reed, J. Rohlf, K. Salyer, D. Sperka, D. Spitzbart, I. Suarez, A. Tsatsos, E. Wurtz, A.G. Zecchinelli

Northeastern University, Boston, Massachusetts, USA
A. Aarif, G. Alverson, E. Barberis, J. Bonilla, B. Bylsma, M. Campana, J. Dervan, Y. Haddad, Y. Han, I. Israr, A. Krishna, M. Lu, N. Manganelli, R. Mccarthy, D.M. Morse, T. Orimoto, L. Skinnari, C.S. Thoreson, E. Tsai, D. Wood

Massachusetts Institute of Technology, Cambridge, Massachusetts, USA
C. Baldenegro Barrera, H. Bossi, S. Bright-Thonney, I.A. Cali, Y.c. Chen, P.c. Chou, M. D'Alfonso, J. Eysermans, C. Freer, G. Gomez Ceballos, M. Goncharov, G. Grosso, P. Harris, D. Hoang, G.M. Innocenti, K. Ivanov, D. Kovalskyi, J. Krupa, L. Lavezzo, Y.J. Lee, K. Long, C. Mcginn, A. Novak, M.I. Park, C. Paus, C. Reissel, C. Roland, G. Roland, S. Rothman, T.a. Sheng, G. Stephans, D. Walter, J. Wang, Z. Wang, B. Wyslouch, T. Yang

Wayne State University, Detroit, Michigan, USA
S. Bhattacharya, P.E. Karchin

University of Minnesota, Minneapolis, Minnesota, USA
A. Alpana, B. Crossman, W.J. Jackson, C. Kapsiak, M. Krohn, D. Mahon, J. Mans,

B. Marzocchi, R. Rusack, O. Sancar, R. Saradhy, N. Strobbe

Bethel University, St. Paul, Minnesota, USA
J.M. Hogan

University of Nebraska-Lincoln, Lincoln, Nebraska, USA
K. Bloom, D.R. Claes, G. Haza, J. Hossain, C. Joo, I. Kravchenko, K.H.M. Kwok, A. Rohilla, J.E. Siado, W. Tabb, A. Vagnerini, A. Wightman, F. Yan

Rutgers, The State University of New Jersey, Piscataway, New Jersey, USA
B. Chiarito, J.P. Chou, S.V. Clark, S. Donnelly, D. Gadkari, Y. Gershtein, E. Halkiadakis, C. Houghton, D. Jaroslawski, A. Kobert, I. Laflotte, A. Lath, J. Martins, M. Perez Prada, B. Rand, J. Reichert, P. Saha, S. Salur, S. Schnetzer, S. Somalwar, R. Stone, S.A. Thayil, S. Thomas, J. Vora

Princeton University, Princeton, New Jersey, USA
H. Bouchamaoui, G. Dezoort, P. Elmer, A. Frankenthal, M. Galli, B. Greenberg, N. Haubrich, K. Kennedy, G. Kopp, Y. Lai, D. Lange, A. Loeliger, D. Marlow, I. Ojalvo, J. Olsen, F. Simpson, D. Stickland, C. Tully

State University of New York at Buffalo, Buffalo, New York, USA
H. Bandyopadhyay, L. Hay, H.w. Hsia, I. Iashvili, A. Kalogeropoulos, A. Kharchilava, A. Mandal, M. Morris, D. Nguyen, S. Rappoccio, H. Rejeb Sfar, A. Williams, D. Yu

Cornell University, Ithaca, New York, USA
J. Alexander, X. Chen, J. Dickinson, A. Duquette, J. Fan, X. Fan, J. Grassi, S. Hogan, P. Kotamnives, J. Monroy, G. Niendorf, M. Oshiro, J.R. Patterson, A. Ryd, J. Thom, P. Wittich, R. Zou, L. Zygala

University of Rochester, Rochester, New York, USA
O. Bessidskaia Bylund, A. Bodek, P. de Barbaro, R. Demina, A. Garcia-Bellido, H.S. Hare, O. Hindrichs, N. Parmar, P. Parygin[93], H. Seo, R. Taus

The Ohio State University, Columbus, Ohio, USA
M. Carrigan, R. De Los Santos, L.S. Durkin, C. Hill, M. Joyce, D.A. Wenzl, B.L. Winer, B. Yates

Carnegie Mellon University, Pittsburgh, Pennsylvania, USA
J. Alison, S. An, M. Cremonesi, V. Dutta, E.Y. Ertorer, T. Ferguson, T.A. Gómez Espinosa, A. Harilal, A. Kallil Tharayil, M. Kanemura, C. Liu, M. Marchegiani, P. Meiring, S. Murthy, P. Palit, K. Park, M. Paulini, A. Roberts, A. Sanchez, W. Terrill

University of Puerto Rico, Mayaguez, Puerto Rico, USA
S. Malik, R. Sharma

Brown University, Providence, Rhode Island, USA
G. Barone, G. Benelli, D. Cutts, S. Ellis, L. Gouskos, M. Hadley, U. Heintz, K.W. Ho, T. Kwon, L. Lambrecht, G. Landsberg, K.T. Lau, J. Luo, S. Mondal, J. Roloff, T. Russell, S. Sagir[94], X. Shen, M. Stamenkovic, N. Venkatasubramanian

University of Tennessee, Knoxville, Tennessee, USA
D. Ally, A.G. Delannoy, S. Fiorendi, J. Harris, T. Holmes, A.R. Kanuganti,

N. Karunarathna, J. Lawless, L. Lee, E. Nibigira, B. Skipworth, S. Spanier

Vanderbilt University, Nashville, Tennessee, USA
E. Appelt, Y. Chen, S. Greene, A. Gurrola, W. Johns, R. Kunnawalkam Elayavalli, A. Melo, D. Rathjens, F. Romeo, P. Sheldon, S. Tuo, J. Velkovska, J. Viinikainen, J. Zhang

Texas A&M University, College Station, Texas, USA
D. Aebi, M. Ahmad, T. Akhter, K. Androsov, A. Basnet, A. Bolshov, O. Bouhali[95], A. Cagnotta, V. D'Amante, R. Eusebi, P. Flanagan, J. Gilmore, Y. Guo, T. Kamon, S. Luo, R. Mueller, A. Safonov

Rice University, Houston, Texas, USA
D. Acosta, A. Agrawal, C. Arbour, T. Carnahan, P. Das, K.M. Ecklund, F.J. Geurts, T. Huang, I. Krommydas, N. Lewis, W. Li, J. Lin, O. Miguel Colin, B.P. Padley, R. Redjimi, J. Rotter, C. Vico Villalba, M. Wulansatiti, E. Yigitbasi, Y. Zhang

Texas Tech University, Lubbock, Texas, USA
N. Akchurin, J. Damgov, Y. Feng, N. Gogate, W. Jin, Y. Kazhykarim, K. Lamichhane, S.W. Lee, C. Madrid, A. Mankel, T. Peltola, I. Volobouev

Baylor University, Waco, Texas, USA
S. Abdullin, A. Brinkerhoff, E. Collins, M.R. Darwish, J. Dittmann, K. Hatakeyama, V. Hegde, J. Hiltbrand, B. McMaster, J. Samudio, S. Sawant, C. Sutantawibul, J. Wilson

University of Virginia, Charlottesville, Virginia, USA
B. Cardwell, H. Chung, B. Cox, J. Hakala, G. Hamilton Ilha Machado, R. Hirosky, M. Jose, A. Ledovskoy, C. Mantilla, C. Neu, C. Ramón Álvarez, Z. Wu

University of Wisconsin - Madison, Madison, Wisconsin, USA
A. Aravind, S. Banerjee, K. Black, T. Bose, E. Chavez, S. Dasu, P. Everaerts, C. Galloni, H. He, M. Herndon, A. Herve, C.K. Koraka, S. Lomte, R. Loveless, A. Mallampalli, A. Mohammadi, S. Mondal, T. Nelson, G. Parida, D. Pinna, L. Pétré, A. Savin, V. Shang, V. Sharma, W.H. Smith, D. Teague, H.F. Tsoi, W. Vetens, A. Warden

[1]Also at Yerevan State University, Yerevan, Armenia
[2]Also at Technische Universität Wien, Vienna, Austria
[3]Also at Ghent University, Ghent, Belgium
[4]Also at FACAMP - Faculdades de Campinas, Sao Paulo, Brazil
[5]Also at Universidade Estadual de Campinas, Campinas, Brazil
[6]Also at Federal University of Rio Grande do Sul, Porto Alegre, Brazil
[7]Also at The University of the State of Amazonas, Manaus, Brazil
[8]Also at University of Chinese Academy of Sciences, Beijing, China
[9]Also at University of Chinese Academy of Sciences, Beijing, China
[10]Also at School of Physics, Zhengzhou University, Zhengzhou, China
[11]Now at Henan Normal University, Xinxiang, China
[12]Also at University of Shanghai for Science and Technology, Shanghai, China
[13]Also at The University of Iowa, Iowa City, Iowa, USA
[14]Also at Nanjing Normal University, Nanjing, China
[15]Also at Center for High Energy Physics, Peking University, Beijing, China, Beijing, China

[16]Also at Cairo University, Cairo, Egypt
[17]Also at British University in Egypt, Cairo, Egypt
[18]Now at Ain Shams University, Cairo, Egypt
[19]Also at Purdue University, West Lafayette, Indiana, USA
[20]Also at Université de Haute Alsace, Mulhouse, France
[21]Also at Ilia State University, Tbilisi, Georgia
[22]Also at Joint Institute for Nuclear Research, Dubna, Russia
[23]Also at University of Hamburg, Hamburg, Germany
[24]Also at RWTH Aachen University, III. Physikalisches Institut A, Aachen, Germany
[25]Also at Bergische University Wuppertal (BUW), Wuppertal, Germany
[26]Also at Brandenburg University of Technology, Cottbus, Germany
[27]Also at Institute for Advanced Simulation - Jülich Supercomputing Centre, Juelich, Germany
[28]Also at CERN, European Organization for Nuclear Research, Geneva, Switzerland
[29]Also at HUN-REN ATOMKI - Institute of Nuclear Research, Debrecen, Hungary
[30]Now at Universitatea Babes-Bolyai - Facultatea de Fizica, Cluj-Napoca, Romania
[31]Also at MTA-ELTE Lendület CMS Particle and Nuclear Physics Group, Eötvös Loránd University, Budapest, Hungary
[32]Also at HUN-REN Wigner Research Centre for Physics, Budapest, Hungary
[33]Also at Physics Department, Faculty of Science, Assiut University, Assiut, Egypt
[34]Also at The University of Kansas, Lawrence, Kansas, USA
[35]Also at Punjab Agricultural University, Ludhiana, India
[36]Also at University of Hyderabad, Hyderabad, India
[37]Also at Indian Institute of Science (IISC), Bangalore, India
[38]Also at University of Visva-Bharati, Santiniketan, India
[39]Also at Institute of Physics, Bhubaneswar, India
[40]Also at Deutsches Elektronen-Synchrotron, Hamburg, Germany
[41]Also at Isfahan University of Technology, Isfahan, Iran
[42]Also at Sharif University of Technology, Tehran, Iran
[43]Also at Department of Physics, University of Science and Technology of Mazandaran, Behshahr, Iran
[44]Also at Department of Physics, Faculty of Science, Arak University, ARAK, Iran
[45]Also at Helwan University, Cairo, Egypt
[46]Also at Italian National Agency for New Technologies, Energy and Sustainable Economic Development, Bologna, Italy
[47]Also at Centro Siciliano di Fisica Nucleare e di Struttura della Materia, Catania, Italy
[48]Also at James Madison University, Harrisonburg, Virginia, USA
[49]Also at Università degli Studi Guglielmo Marconi, Roma, Italy
[50]Also at Scuola Superiore Meridionale, Università di Napoli 'Federico II', Napoli, Italy
[51]Also at Fermi National Accelerator Laboratory, Batavia, Illinois, USA
[52]Also at Laboratori Nazionali di Legnaro dell'INFN, Legnaro, Italy
[53]Also at Lulea University of Technology, Lulea, Sweden
[54]Also at Consiglio Nazionale delle Ricerche - Istituto Officina dei Materiali, Perugia, Italy
[55]Also at UPES - University of Petroleum and Energy Studies, Dehradun, India
[56]Also at Institut de Physique des 2 Infinis de Lyon (IP2I), Villeurbanne, France
[57]Also at Department of Applied Physics, Faculty of Science and Technology, Universiti Kebangsaan Malaysia, Bangi, Malaysia
[58]Also at Yerevan Physics Institute, Yerevan, Armenia
[59]Also at Imperial College, London, United Kingdom
[60]Also at California Institute of Technology, Pasadena, California, USA

[61]Also at Trincomalee Campus, Eastern University, Sri Lanka, Nilaveli, Sri Lanka
[62]Also at Saegis Campus, Nugegoda, Sri Lanka
[63]Also at National and Kapodistrian University of Athens, Athens, Greece
[64]Also at Ecole Polytechnique Fédérale Lausanne, Lausanne, Switzerland
[65]Also at St. Petersburg Polytechnic University, St. Petersburg, Russia
[66]Also at Universität Zürich, Zurich, Switzerland
[67]Also at Stefan Meyer Institute for Subatomic Physics (SMI), Vienna, Austria
[68]Also at Near East University, Research Center of Experimental Health Science, Mersin, Türkiye
[69]Also at Konya Technical University, Konya, Türkiye
[70]Also at Istanbul Topkapi University, Istanbul, Türkiye
[71]Also at Izmir Bakircay University Faculty of Engineering and Architecture, Izmir, Türkiye
[72]Also at Adiyaman University, Adiyaman, Türkiye
[73]Also at Bozok Universitetesi Rektörlügü, Yozgat, Türkiye
[74]Also at Istanbul Sabahattin Zaim University, Istanbul, Türkiye
[75]Also at Marmara University, Istanbul, Türkiye
[76]Also at Milli Savunma University, Naval Academy, Istanbul, Türkiye
[77]Also at The Science and Technological research Council of Türkiye, Informatics and Information Security Research Center, Gebze/Kocaeli, Türkiye
[78]Also at Kafkas University, Kars, Türkiye
[79]Now at Istanbul Okan University, Istanbul, Türkiye
[80]Also at Istanbul University - Cerrahpasa, Faculty of Engineering, Istanbul, Türkiye [81]Also at Istinye University Vadi Campus, Ayazağa District Azerbaijan Street (Vadistanbul 4A) Sarıyer, İstanbul, Türkiye
[82]Also at School of Physics and Astronomy, University of Southampton, Southampton, United Kingdom
[83]Also at Monash University, Faculty of Science, Clayton, Australia
[84]Also at Università di Torino, Torino, Italy
[85]Also at California Lutheran University, Thousand Oaks, California, USA
[86]Also at United States Naval Academy - Physics Department, Annapolis, Maryland, USA
[87]Also at Institute for Nuclear Research, Moscow, Russia
[88]Also at Bingol University, Bingol, Türkiye
[89]Also at Georgian Technical University, Tbilisi, Georgia
[90]Also at Sinop University, Sinop, Türkiye
[91]Also at Erciyes University, Kayseri, Türkiye
[92]Also at Horia Hulubei National Institute of Physics and Nuclear Engineering (IFIN-HH), Bucharest, Romania
[93]Now at National Research Nuclear University 'Moscow Engineering Physics Institute' (MEPhI), Moscow, Russia
[94]Also at Karamanoğlu Mehmetbey University, Karaman, Türkiye
[95]Also at Hamad Bin Khalifa University (HBKU), Doha, Qatar